Changes in geographical runoff generation in regions affected by climate and resource development: A case study of the Athabasca River

Peters, D. L., Watt, D., Devito, K., Monk, W. A., Shrestha, R. R., & Baird, D. J.

2022

Journal of Hydrology: Regional Studies 39 (2022) 100981

Contents lists available at ScienceDirect

Journal of Hydrology: Regional Studies

journal homepage: www.elsevier.com/locate/ejrh

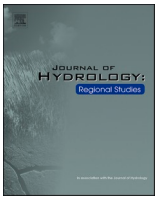

Changes in geographical runoff generation in regions affected by climate and resource development: A case study of the Athabasca River

Daniel L. Peters [a,b,*], Dillon Watt [b], Kevin Devito [c], Wendy A. Monk [d], Rajesh R. Shrestha [a,b], Donald J. Baird [e]

[a] *Environment and Climate Change Canada, University of Victoria Queenswood Campus, 2474 Arbutus Road, Victoria, British Columbia V8N 1V8, Canada*
[b] *Department of Geography, University of Victoria, Victoria, British Columbia, Canada*
[c] *Department of Biology, University of Alberta, Edmonton, Alberta, Canada*
[d] *Environment and Climate Change Canada @ Canadian Rivers Institute, Faculty of Forestry and Environmental Management, University of New Brunswick, Fredericton, New Brunswick, Canada*
[e] *Environment and Climate Change Canada @ Canadian Rivers Institute, Department of Biology, University of New Brunswick, Fredericton, New Brunswick, Canada*

ARTICLE INFO

Keywords:
Runoff generation
Trend analysis
Relative flow contributions
Basin geography
Hydrological indicators, oil sands region

ABSTRACT

Study region: This study is focused on the lower Athabasca Basin in northwestern Canada that has experienced rapid expansion of oil sands development.
Study focus: The goal of this study is to enhance the understanding of the regional role of the lower Athabasca Basin areas in overall runoff delivery to the downstream Peace-Athabasca Delta. The Cold-regions Hydrological Indicators of Change framework was applied to examine key hydro-ecological relevant indicators influencing the delta.
New hydrological insights for the region: Our novel approach yielded new insights that should be considered in water management. Primarily, a combined flow magnitude and relative flow contributions analysis by geography provides an improved understanding of contrasting runoff generation changes, in terms of opposing responses occurring within a basin. For instance, open-water low flows emanated from the upper regions and a generally increasing tendency from the lower regions. Furthermore, peak summer flows generally experienced decreases from the upper and portions of the lower basin, while contrary increasing tendencies emerged for the east bank of the lower Athabasca River mainstem. Moving beyond the traditional approach of looking only at the climate, landscape and geology were considered as potential causal factors for divergent runoff generation responses. Our approach is transferable to other regional studies.

1. Introduction

Variable and changing climatic conditions, land-use change and flow regulation have individually or cumulatively been associated

* Corresponding author at: Environment and Climate Change Canada, University of Victoria Queenswood Campus, 2474 Arbutus Road, Victoria, British Columbia V8N 1V8, Canada.
E-mail address: Daniel.Peters@ec.gc.ca (D.L. Peters).

https://doi.org/10.1016/j.ejrh.2021.100981
Received 6 May 2021; Received in revised form 29 November 2021; Accepted 8 December 2021
Available online 22 December 2021

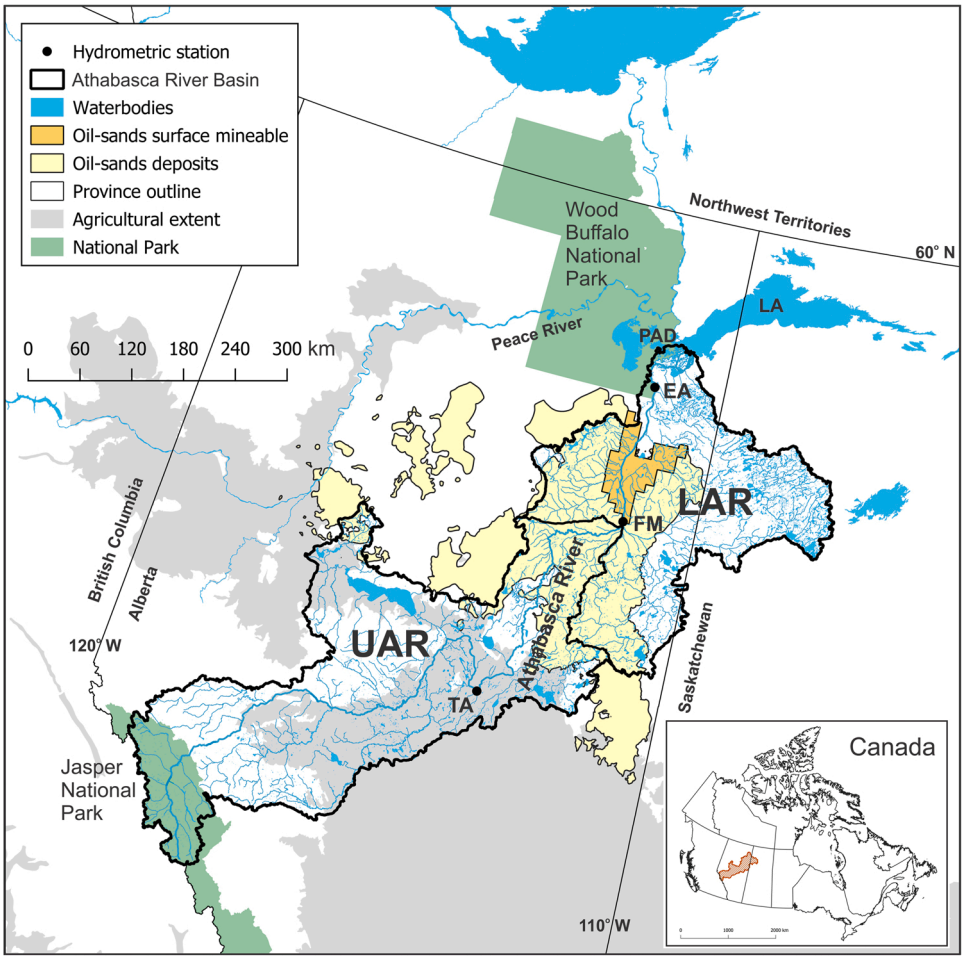

Fig. 1. Athabasca River Basin in western Canada. UAR and LAR are the Upper and Lower Athabasca River drainage areas, respectively. Hydrometric gauges on the Athabasca River mainstem are Town of Athabasca (TA), just below city of Fort McMurray (FM) and at Embarras Airport (EA). The oil sand deposits straddle the UAR/LAR boundary, with surface mineable areas located downstream of FM. The Peace-Athabasca Delta (PAD) and Lake Athabasca (LA) are also shown. Inset map shows location of study basin within western Canada.

with global streamflow regime alterations (Botter et al., 2013; Environment Canada, 2004; Zeiringer et al., 2018). In this context, western Canada has been identified as a region of particular concern regarding altered water availability issues due to climate warming and consequent changes in temperature, snowfall, rainfall and evapotranspiration (Bonsal et al., 2020, 2019). In this region, the Athabasca River is an important water source for oil sands mining projects, and also provides key ecosystem services to the internationally-recognized Peace-Athabasca Delta (PAD) including maintenance of critical habitat for fish, vegetation, wildlife and associated traditional hunting and fishing practices (Timoney, 2013). Schindler and Donahue (2006) postulated an impending crisis of water scarcity in this river system, with potential impacts on environmental flow needs linked to diminishing summer streamflow quantity. In response to this concern, a regional surface water management framework was implemented to address expanding resource development in the lower part of the basin (GoA, 2015). Indigenous Peoples have also raised water quantity concerns in their petition to UNESCO to reassess the protection status of Wood Buffalo National Park (UNESCO, 2017), which includes the PAD.

Investigations into the abrupt decline in post-1950s flow of the Athabasca River highlighted by Schindler and Donahue (2006) revealed that such a decline was not apparent when examining hydrometric records along the mainstem for the upper half of the basin (Peters et al., 2013; Rood et al., 2015). Also, in contrast with declining trends in flow rates entering the lower regions where oil sands mining is occurring (Bawden et al., 2014; Monk et al., 2012; Rasouli et al., 2013; Rood et al., 2015; Schindler and Donahue, 2006), exploratory work by Peters et al. (2013) indicated no discernable trend in runoff from the lowermost portion of the basin (eg, downstream of Athabasca River just below Fort McMurray). The lack of within-basin consensus on runoff generation response tendencies points to potentially divergent responses to multiple drivers, such as climate, water use and landscape alteration.

In addition to climate, cumulative changes in land use and water withdrawal are likely also influencing net contributions to water movement and observed trends in flow of the Athabasca mainstem (Squires et al., 2010) and its tributaries (Bawden et al., 2014). For example, short-term increases in water inputs may be expected with peatland ditching, draining and overburden dewatering for accessing near-surface oil sand deposits (Woynillowicz and Severson-Baker, 2006); while decreases may be expected from water use by

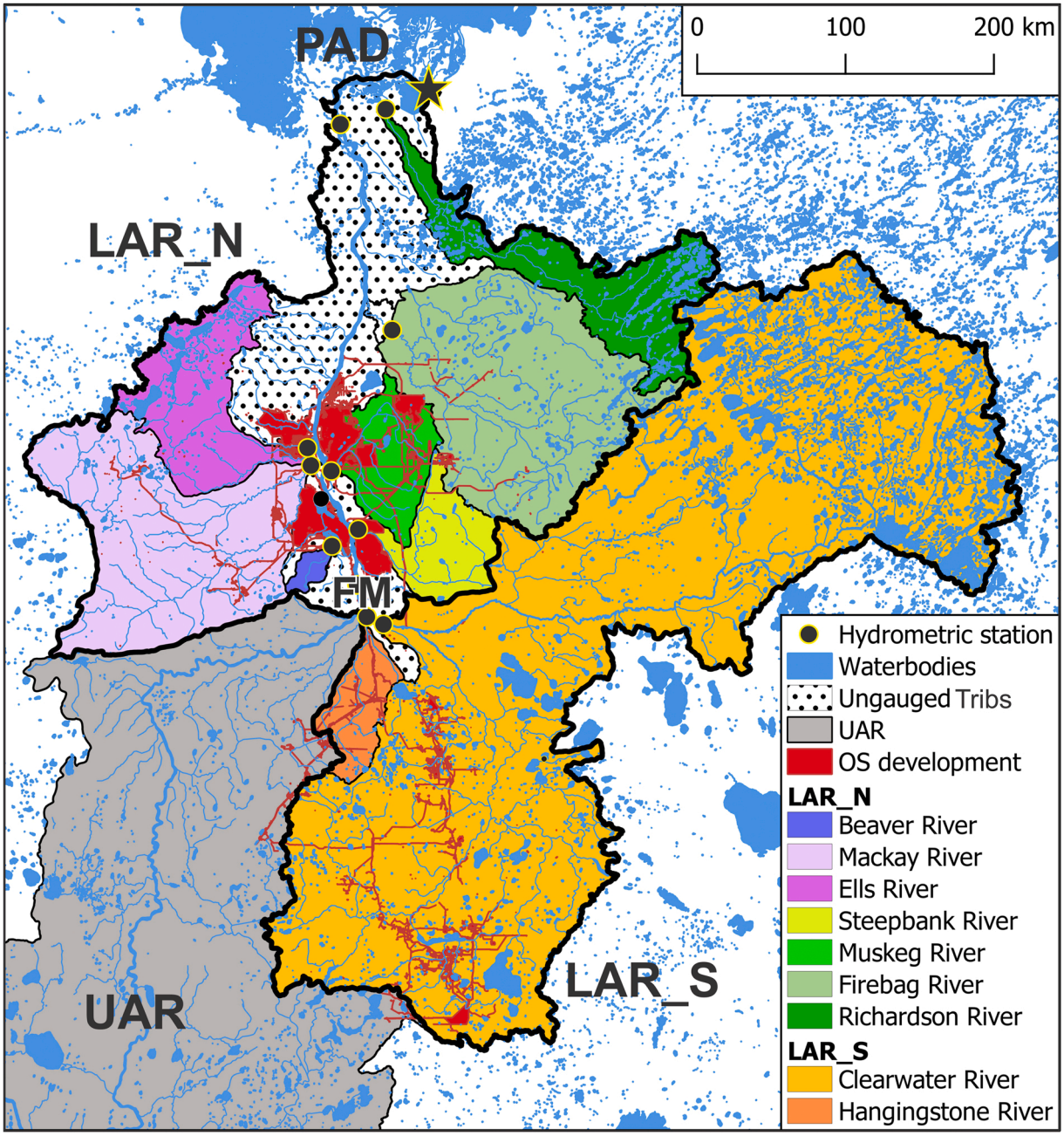

Fig. 2. Lower Athabasca River (LAR) highlighting study basins, gauged tributaries and oil sands (OS) developed areas as of 2017. Note that the Upper Athabasca River (UAR) is upstream of the OS development; While the LAR South (LAR_S) contains in-situ and LAR North (LAR_N) contains both in-situ and open-pit mining development. The star is the most downstream basin area considered in this study delimited by the water level gauge on the Athabasca River near Jackfish Creek in the Peace-Athabasca Delta (PAD). See Table 1 for hydrometric station and basin information.

industry. Long-term influence on hydrology associated with the many disturbances associated with open pit and steam assisted gravity drainage oil extraction, as well as from traditional oil and gas developments and maintenance within the basin (Schneider et al., 2003), may result in potential changes to water partitioning, storage, and hydrological connectivity (Kompanizare et al., 2018).

Previous flow analyses (eg, Alexander and Chambers, 2016; Bawden et al., 2014) and modelling (eg, Eum et al., 2016) suggest that trends in the quantity and/or timing of streamflow variables (eg, peak) resulting from the effects of climate or natural resource development may be present in the hydrometric time series of the lower Athabasca River (LAR), and require further study to gain an understanding of causal factors. Although the general runoff regime is well understood (eg, Peters et al., 2013), there is a knowledge gap regarding the origin of these trends and how the geography of runoff production driving key deltaic hydro-ecological events, such as the spring ice-jam and summer open-water floods, have changed over time.

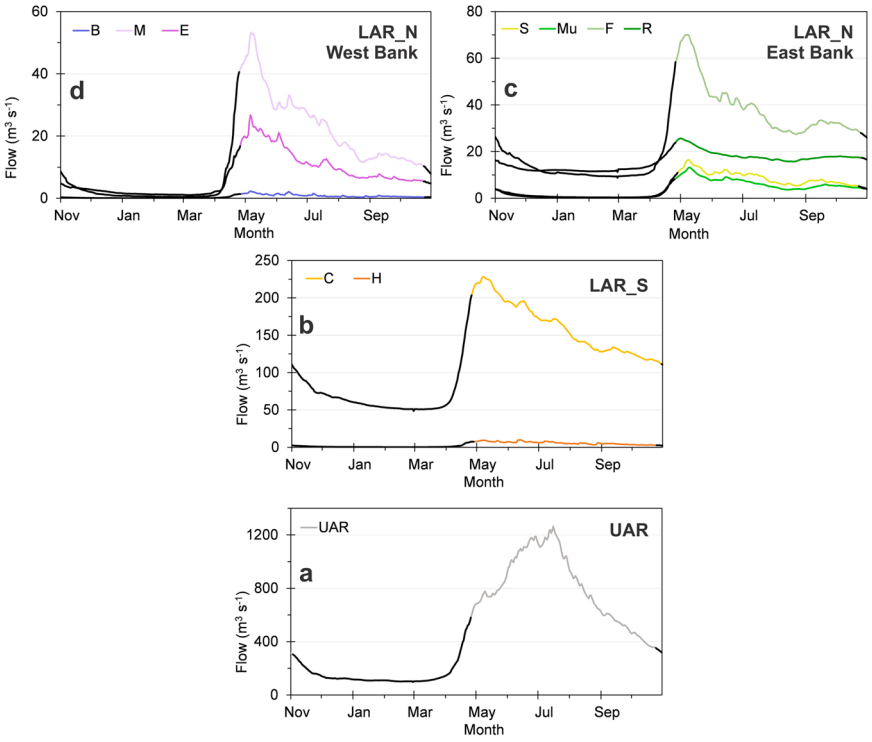

Fig. 3. Mean daily flow regimes for 1974–2017 period: a) Upper Athabasca River (UAR); b) Lower Athabasca River south (LAR_S) comprised of Clearwater (C) and Hangingstone Rivers (H); c) Lower Athabasca River North (LAR_N) East Bank comprised of Steepbank, (S) Muskeg (Mu), Firebag (F) and Richardson (R) Rivers; d) LAR_N West Bank comprised of Beaver (B), Mackay (M) and Ells (E) Rivers. Note that November to February mean flow in LAR_N were based on < 44 years of data (see Table 1). Ice covered period of the flow depicted with a dark line. The flow regime order presentation and colours correspond to the order presented in the text and to the sub-basin geography and colours of the tributaries presented in Fig. 2.

Here we present a novel approach that explicitly considers the importance of contributions from the lower Athabasca Basin, where oil sands mining is concentrated, to total flow generation during ice and open-water conditions. In this context, the goal of this study was to assess potential changes in streamflow generation in tributaries draining the LAR basin by applying the Cold-regions Hydrological Indicators of Change (CHIC) framework (Peters et al., 2014). Furthermore, distinct runoff generation pathways from upstream and downstream portions of the basin were considered to gain an improved understanding of regional contributions to ecologically-important flows driving the downstream PAD ecosystem.

2. Study area

The Athabasca River (~159,000 km^2) is the largest direct inflow to the PAD and Lake Athabasca system in northwestern Canada (Figs. 1 and 2), originating in the Columbia Icefields in the Rocky Mountains, and draining eight physiological sub-regions of Alberta (Downing and Pettapiece, 2006). The river travels through the rugged alpine, sub-alpine and forested montane natural sub-regions of Jasper National Park, further through foothills and onto the low relief, mixed wood forest of the Boreal Plains. Low flows associated with these upper regions of the basin are ~100–200 m^3 s^{-1} during the ice-covered months, while peak flows range from ~1000 up to < 5000 m^3 s^{-1} in response to the spring freshet and summer rainfall events (Peters and Prowse, 2006).

At Fort McMurray, the Hangingstone (Boreal highlands) and Clearwater (Athabasca plains and Boreal shield) Rivers join the mainstem. The Steepbank, Muskeg, Mackay, Firebag and Richardson Rivers drain the nearby hills, with a strong spring freshet signal to the flow regimes influencing the downstream delta (Fig. 3). The downstream PAD is a wetland ecosystem of international significance recognized by the Ramsar Convention and 80% lies within the Wood Buffalo National Park (a UNESCO World Heritage site).

Agricultural, oil and gas, and forestry related land-use change activities are present within the basin (NRBS, 1996). Several pulp mills are located on the river between the town of Hinton and Athabasca, and oil sand mining occurs near Fort McMurray. Landscape alteration associated with open-pit mining of the oil sands commenced in the late 1960s. Approximately 767 km^2 of the 4800 km^2 available for surface mining have been disturbed as of 2017 (GoA, 2019) (Fig. 1 and Table 1). Less than 5% of the annual river flow is allocated for water use; withdrawals by the oil sands industry comprise the bulk of this allocation (GoA, 2015).

Table 1
Hydrometric information (ECCC, 2020) for key Athabasca River mainstem stations shown in Fig. 1. Geographic information for study area presented in Fig. 2, including gauged and ungauged areas, oil-sands mining type (in situ and/or open pit) and start of activities with years of early/late development and % basin area affected as of the end of 2017.

Basin Area / Station Name	Station ID	Record Years	Drainage Area km^2	% of Total Basin Area	Oil Sands Mining Type Year Early & Late Development	% Basin Area Affected by Development[d]
Athabasca River at Athabasca	07BE001	1913–31, 1938–2017	73,300	46.1		
Athabasca River below Ft McMurray	07DA001	1958–2017	132,588	83.4		
Athabasca River at Embarras Airport	07DA001	1971–87, 2014–2017	153,000	96.2		
Upper Athabasca River Basin			**100,000**	**62.9**		
Athabasca River at Ft McMurray	07CC002	1958–2017**				
Lower Athabasca River Basin South			**31,900**	**20.1**		
Clearwater River at Draper	07CD001	1930–2017[R]	30,792	19.4	In situ, 1997, 2002	0.5
Hangingstone River at Ft McMurray	07CD004	1965 – 2017	962	0.6	In situ, 1999	1.6
Ungauged Areas			146	0.1		
Lower Athabasca River Basin North			**27,100**	**17**		
Steepbank River near Ft McMurray	07DA006	1972–2017*	1320	0.8	Surface, 1994, 2001	
Muskeg River near Ft MacKay	07DA008	1974–2017*	1457	0.9	Surface, 1996, 2002	16.4
Beaver River above Syncrude	07DA018	1975 – 2017[a,b]	165	0.1		
MacKay River near Ft MacKay	07DB001	1972–2017*	5569	3.5	Both, 1978, 2002	0.9
Ells River near Ft Mackay / ab. CNRL Bridge	07DA17 / S14A	1975 – 1986,[c],2001 – 2017	2450	1.5	In situ, 1978, 2015	1.6
Firebag River near the Mouth	07DC001	1970–2017*	5988	3.8	In situ, 1987, 2004	1.3
Richardson River near the Mouth	07DD002	1970–2017*[R]	2731	1.7		
Ungauged Areas			7420	4.7	Surface	??
Total Athabasca River Basin			**159,000**	**100**		

R Reference Hydrometric Basin Network station
*Seasonal March to October data for period 1987–2012
**Estimate flow derived by subtracting Clearwater and Hangingstone Rivers from Athabasca River just below Ft McMurray station
[a] Unit area corrected runoff for 1974–75 period from Beaver River near Ft Mackay (07DA005) were merged with Beaver River above Syncrude
[b] Regional Aquatic Monitoring Program (RAMP, 2018) station data
[c] Missing data filled-in using regression equation developed by Alberta Environment (Seneka, 2002) with adjacent Mackay River.
[d] 2014 GIS information % area affected by oil sands mining of RAMP (2016) updated to year 2017 using Human Footprint Data Inventory of ABMI (2020)

3. Methods

3.1. Hydrometric data sources

Observed mean daily flows ($m^3\ s^{-1}$) were obtained for 12 hydrometric stations from the HYDAT archive (ECCC, 2020) (Table 1). Stations at the town of Athabasca (TA) and just below the city of Fort McMurray (FM) represent cumulative runoff generated to the middle and lower portions of the basin. Alberta Environment (Bothe, 1982) estimates of monthly mean flow derived via regression analyses were used to fill in missing data and produce a new 1912–2017 time series for both these stations.

With the exception of the Clearwater and Hangingstone Rivers (> 45 years), tributaries downstream of FM were instrumented in the early 1970s as part of the Alberta Oil Sands Environmental Research Program (AOSERP; Neill and Evans, 1979). The Steepbank, Muskeg, Mackay, Firebag and Richardson River stations were reduced to seasonal gauging (March to October) between 1987 and 2013. The Beaver River headwaters were altered by oil sands operations, and thus a unit area runoff correction was applied to incorporate the 1974–75 data to the station that was relocated slightly downstream. Gauging of the Ells River was interrupted between 1987 and 2000; missing years were infilled using a regression equation developed by Alberta Environment based on the adjacent Mackay River (Seneka, 2002) and missing ice-affected dates were taken from this river.

Table 2
List of ecologically relevant cold-regions hydrological indicators of changes (CHIC) adapted from Peters et al. (2014) that are used in this study.

	Hydro-ecological variables	Example of ecological influence
Annual	Mean March to October flow (**MOF**)	Water availability
	Date 50% total flow (centre of mass) attained ($\mathbf{CM_d}$)	Shift in water availability timing
	Monthly mean flow magnitude March to October (**Mar to Oct**)	Availability and temporal variability of suitable aquatic and riparian habitat
	Flow magnitude ($\mathbf{FI_Q}$) on day of freshet initiation ($\mathbf{FI_d}$)	Flows that structure aquatic habitat availability and channel morphology through substrate scour and ice jam-associated flooding
Ice Influenced	Date of freeze-up ($\mathbf{FU_d}$) and breakup ($\mathbf{BU_d}$)	Timing of winter ice formation can reduce habitat availability and alter distribution. Loss of ice related to habitat availability and cues for spawning
	Magnitude of flow at freeze-up ($\mathbf{FU_Q}$) and breakup ($\mathbf{BU_Q}$)	Magnitude of flow at time of freeze-up can be directly related to loss of shallow water habitat and reduction in the dilution of contaminants
	Date of maximum water level during ice influenced period ($\mathbf{HM_d}$)	Timing important for connectivity
	Flow magnitude on day of ice influenced maximum water level ($\mathbf{HM_Q}$)	Related to habitat availability especially channel connectivity
Open Water	Date of 1-day low open-water flow ($\mathbf{LO_d}$)	Timing of short-term extreme low flow conditions can influence aquatic spawning
	1-day low open-water flow magnitude ($\mathbf{LO_Q}$)	Short-term extreme low flow conditions affect habitat availability
	Date of 1-day peak flow prior to ($\mathbf{P1_d}$) and after ($\mathbf{P2_d}$) June 1st	Timing of short-term extreme peak flow conditions can influence life cycles
	1-day peak flow magnitude prior to ($\mathbf{P1_Q}$) and after ($\mathbf{P2_Q}$) June 1st	Short-term extreme low flow conditions affect habitat availability
	Mean 90-day peak flow magnitude ($\mathbf{P90_Q}$)	Seasonal low and high flows affect availability of aquatic and riparian habitat

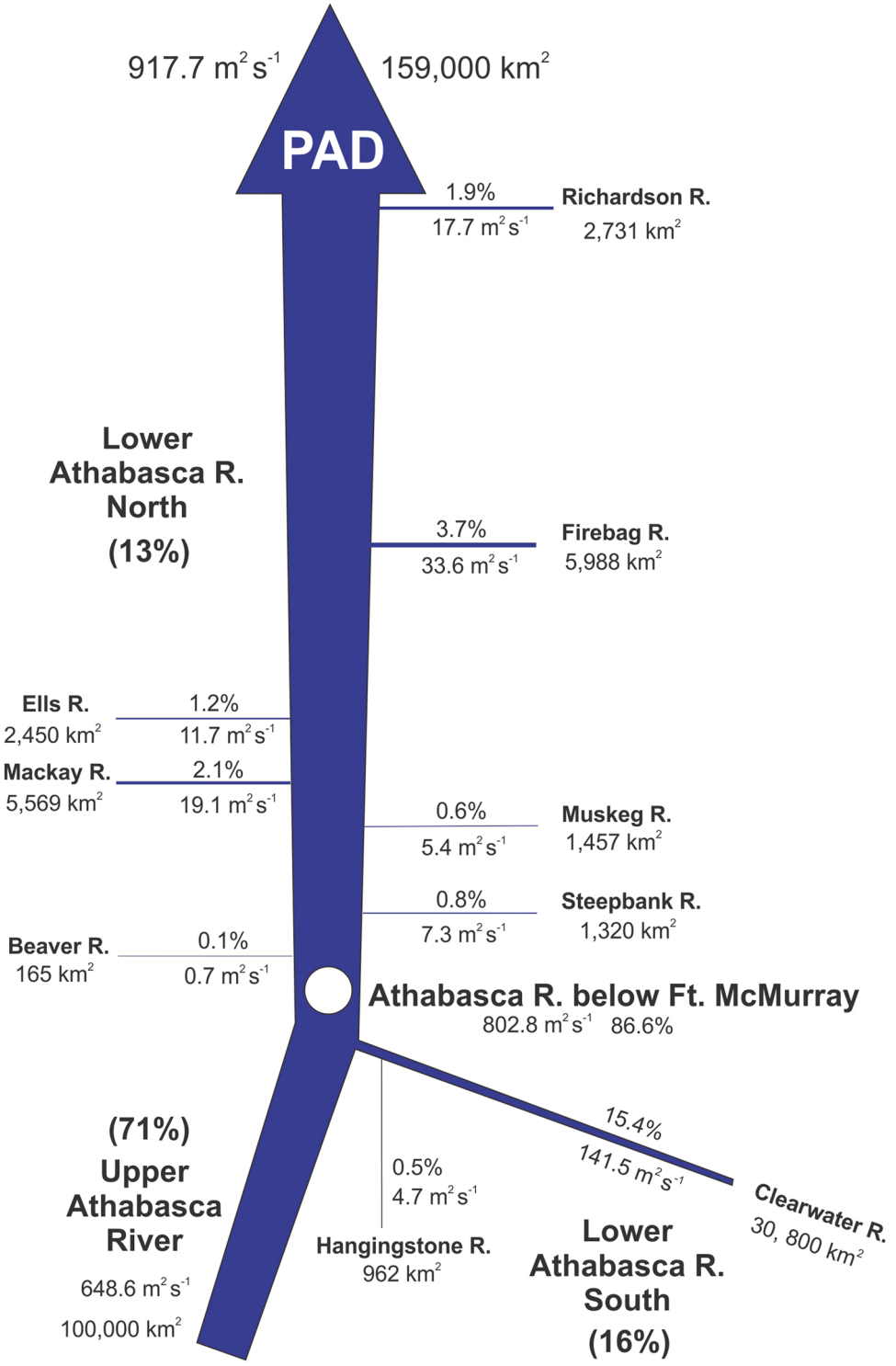

Fig. 4. Mean March to October flow (MOF) balance for the lower Athabasca River Basin area delivering water to the Peace-Athabasca Delta (PAD) based on 1974–2017 data. Data presented are sub basin area, MOF and % of total basin MOF.
Modified from Neill and Evans (1979).

Station data availability and infilling details for the main study years spanning 1974–2017 and focused on March to October flow (MOF) period are outlined in Table 1. This "annual" period (MOF) represents the bulk of the yearly flow regime that captured ice breakup and open-water events.

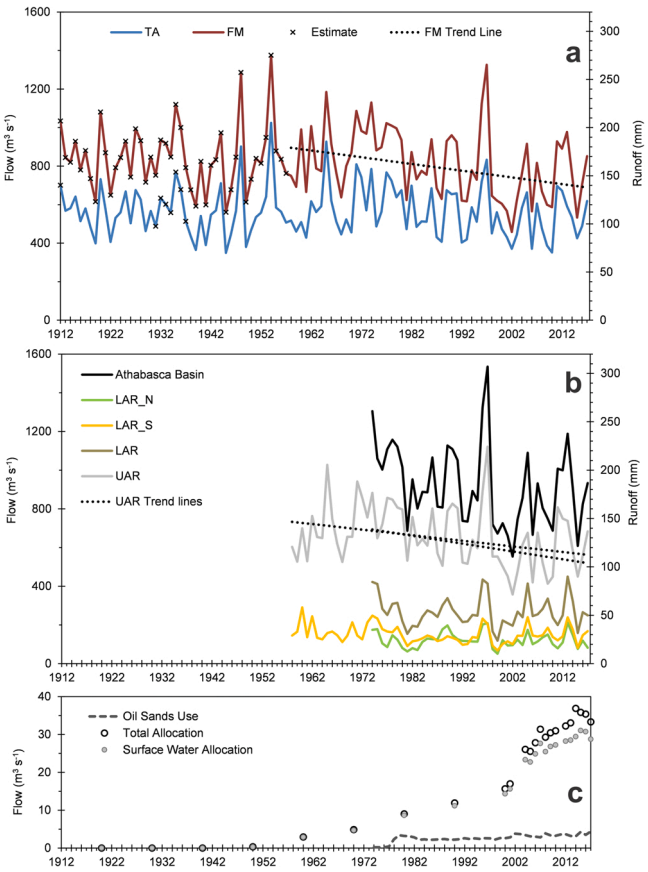

Fig. 5. Mean annual March to October flow (MOF): a) measured on the Athabasca River at town of Athabasca (TA) and just below Fort McMurray (FM) (Bothe, 1982; ECCC, 2020); b), emanating from the Upper Athabasca River (UAR) and flowing through the lower Athabasca River (LAR), addition of flow from the Clearwater and Hangingstone Rivers (LAR_S) at FM, and additions of tributary flow to the LAR below FM (LAR_N; Steepbank, Muskeg, Mackay, Ells, Firebag, Richardson Rivers, plus ungagged areas); c) water use by oil sands industry and watershed scale mean annual allocations for all sectors (AEP, 2019; AER, 2019). Only trend lines significant at $p \leq 0.10$ are plotted: FM (1958–2017) and UAR (1958–2017 & 1974–2017).

3.2. Geographical flow balance

The study basin was separated into two major zones: upper Athabasca River (UAR) and lower Athabasca River (LAR) (Fig. 1 and Table 1). The LAR was sub-divided into southern (LAR_S) and northern (LAR_N) sectors. The LAR_S comprises the of Clearwater River, with minor additions from the Hangingstone River and < 1% ungauged areas. A unique time series of streamflow for the UAR was derived by subtracting the LAR_S flow from those at the contiguous FM hydrometric station. Total flows from the LAR_N region (72% gauged) were produced by adding measured flows on the east bank (gauged via Beaver, Mackay and Ells Rivers) and west bank (gauged via Steepbank, Muskeg, Firebag and Richardson Rivers) to unit area flow extrapolations (1.315 X LAR_N total areas gauged) to account for ungauged areas. This simple method yielded flow values that were within +/−10% of those measured on the Athabasca River at Embarras Airport for the available years 1971–84 and 2014–2017. Due to a lack of continuous daily observed flows at this station near the mouth of the river entering the PAD, total basin analyses that included these extrapolated estimates were restricted to MOF and monthly flows indices, and short timescale indices were referenced to FM.

3.3. Hydrological Indicators

Peters et al. (2014) adapted the Indicators of Hydrologic Alteration (IHA; TNC, 2007) for cold regions to incorporate the effect of ice and snow processes on flow regimes and related ecology (Monk et al., 2018; Peters et al., 2016) through the Cold-regions Hydrological Indicators of Change (CHIC) framework. The CHIC framework quantifies five components of the hydrological regime spanning the ice and open-water periods; namely magnitude, duration, timing, frequency and rate of change of events. The time periods when flows were affected by open-water conditions were separated by considering the 'B' (backwater) flag designation in the HYDAT database (ECCC, 2020) to identify the first and last day when channel hydraulics were affected by ice. Given that the study season was focused on the March 1st to October 31st period, not all CHIC variables were extracted (Table 2).

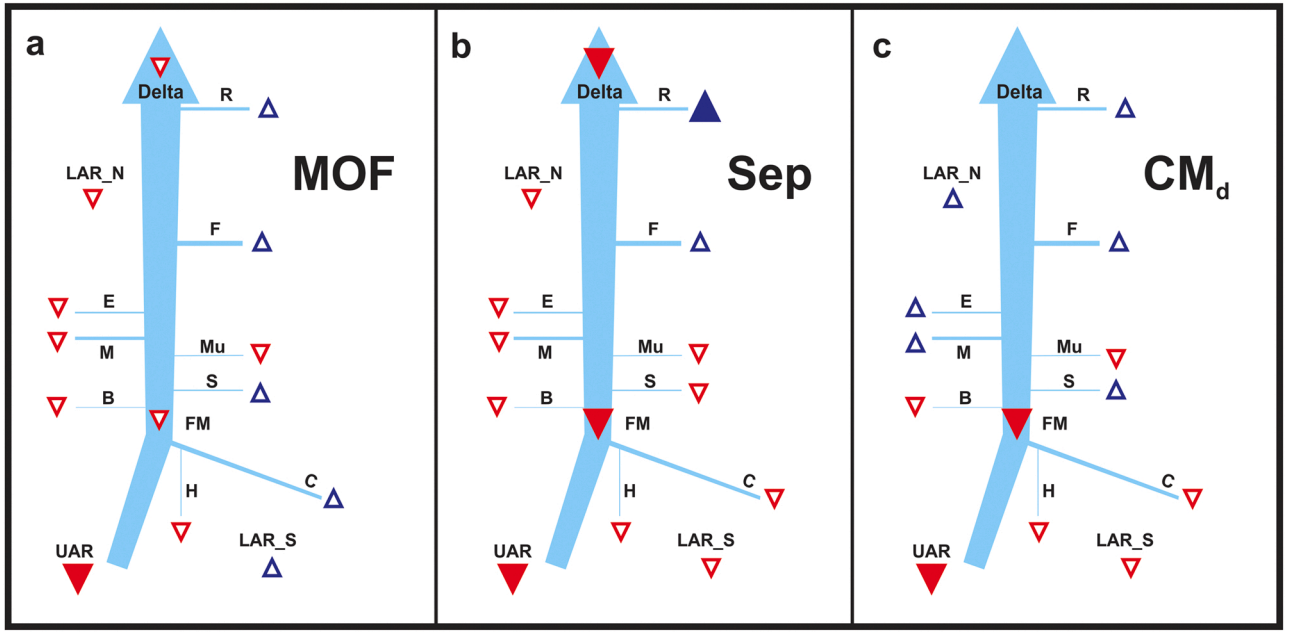

Fig. 6. Results for select trend analyses spanning 1974 – 2017: a) March to October (MOF) mean flow; b) September (Sep) mean flow; c) Centre of mass date (CM_d). UAR- Upper Athabasca River; LAR_S - Lower Athabasca River South; LAR_N – Lower Athabasca River North; AR_FM – Athabasca River just below Fort McMurray; B -Beaver; M – Mackay; E – Ells; H – Hangingstone; C- Clearwater; S -Steepbank; Mu – Muskeg; F – Firebag; and R – Richardson River. Red triangles are decreasing and blue triangles are increasing tendencies, with significant trends ($p \leq 0.10$) depicted by filled in triangles. (For interpretation of the references to colour in this figure legend, the reader is referred to the web version of this article.)

Breakup information was typically available, but on some occasions, a slightly later than usual freeze-up date was not captured prior to gauge removal; in these few cases, October 31 was assigned as the end of the open-water period. The date of the spring freshet initiation (FI_d), with corresponding flow magnitude (FI_Q), was identified as the first notable rise in the hydrograph. Building on the work of Peters and Prowse (2006), the date of the maximum water level (HM_d) influenced by backwater flow conditions (ice) on the Athabasca River, along with the corresponding daily flow magnitude (HM_Q), were extracted for the mainstem hydrometric station located just below FM; this information was not available at the other stations (see de Rham et al., 2020). For all basins, the date (d) and corresponding flow magnitude (m) were extracted for the following indices: river ice breakup (BU_d & BU_Q), centre of mass date (CM_d), mean March to October flow (MOF), mean monthly flow (Mar, Apr, May, Jun, Jul, Aug, Sep and Oct), open-water condition one day low flow date & magnitude (LO_d & LO_Q), peak flow date & magnitude prior to ($P1_d$ & $P1_Q$) and after June 1st ($P2_d$ & $P2_Q$), and the 90-day mean peak flow date and magnitude ($P90_d$ & $P90_Q$). Readers are referred to Richter et al. (1996), Peters and Prowse (2006), TNC (2007) and Peters et al. (2014) for details on the calculations of these variables.

To consider intra-basin (geographical) responses and change over time, we expanded upon other hydrological indicator assessment studies of runoff generation (e.g. Monk et al., 2012; Bawden et al., 2014), and assessed the relative flow (%) contribution from the UAR, LAR_S and LAR_N regions to extreme ice influenced backwater (potential spring ice-jam flood events) and open-water peak flow events (flashy and sustained).

3.4. Statistical analyses

The strength and direction of possible trends in hydrological indicators were assessed using the non-parametric Mann-Kendall (M-K) trend test (Kendall, 1975; Mann, 1945), which has been commonly applied in hydrological and climatological research (e.g. Burn and Hag Elnur, 2002; Monk et al., 2011). M-K trend tests were performed in R (Version 3.6.1; R Development Core Team, 2016) by using the *zyp* package of Bronaugh and Werner (2019), with Zhang and Zwiers (2004) iteratively pre-whitening (IPW) method applied to remove significant serial autocorrelation in the time series (Bürger, 2017; Zhang et al., 2000). The non-parametric slope (β) of each time series was calculated using Sen's estimate (Sen, 1968). Given that the goal of this study was to search for indications of runoff generation change, significant trends were identified at $p \leq 0.10$ (Bawden et al., 2014; Burn et al., 2010; Monk et al., 2012, 2011; Peters et al., 2013). To facilitate comparison with other studies, results at $p \leq 0.05$ were highlighted with an underline in the text. The results of the M-K trend tests (β and p values) are presented in Table A1 to 24 in Appendix A. As previously done by other studies and to maximize the use of available data (eg, Bawden et al., 2014; Peters et al., 2013), the time series analyses were carried out for the 1913–2017, 1958–2017 and 1974–2017 time periods.

4. Results and discussion

4.1. Geographical flow balance

A geographical flow analysis revealed that the combined LAR (37% of the total contributing area) produced ~29% of the long-term mean March to October flow (hereafter MOF) of the Athabasca River basin for the years spanning 1974–2017. The bulk of MOF (~71%) emanated from the Boreal Plains, foothill and mountain regions upstream (63% by area) of the city of Fort McMurray (FM; Fig. 4). The FM hydrometric station includes runoff generated from the LAR_S basin draining the lake-rich Boreal Shield areas which produced only~16% of the total flow but comprises 20% of the total basin area. About 13% of the total flow was generated from the Athabasca Plains areas on both banks of the LAR_N feeding the mainstem downstream of FM. Although generally not as productive as the UAR, the LAR_S and LAR_N represent important water sources likely playing a role in driving components of the hydrograph (ie, indicators) that have yet to be fully addressed in a basin-scale context.

4.2. March 1 to October 31 period indicators

Variability in MOF observed in the last 45 years of record at the Town of Athabasca (TA) and FM were within the range experienced from 1912 to 2017 (Fig. 5a). Although a slight decline in MOF is perceptible over the last century, there was no statistically notable ($p > 0.10$) monotonic trend at both TA and FM gauging locations. These results are in broad agreement with Chen and Grasby (2014) and Rood et al. (2015) who reconstructed mean annual flows back to 1918 and 1937, respectively, via empirical models.

Further investigation of flows from 1958 or 1974–2017 illustrates the relative importance of the UAR and LAR to the total basin flows that enter the delta (Fig. 5b). A significant decrease ($\beta = -2.89$ m^3 s^{-1} y^{-1}) in MOF from the UAR was found post-1958, with a higher decline rate since 1974 ($\beta = -4.05$ m^3 s^{-1} y^{-1}) in line with Schindler and Donahue (2006). In contrast, no significant trends in MOF were observed in either the LAR_S or LAR_N, indicating that overall their proportional contribution to the basin flow at the delta has gradually increased for this time period (Figs. 5b and 6a).

The importance of the LAR to total flow is further emphasized when considered as a percentage of basin-scale streamflow generation over time. From 1974–2017, MOF emanating from the UAR varied from 55% to 82% ($\bar{X} = 71\%$) of the total basin and significantly decreased ($\beta = -0.19\%$ y^{-1}). The proportion to the total basin MOF emanating from the LAR, however, varied between 18% and 45% ($\bar{X} = 29\%$) and significantly increased ($\beta = 0.19\%$ y^{-1}) over this period.

On a monthly basis, significant and notable decreases in mean flow post-1958 for the UAR emerged for Jul ($\beta = -5.8$ m^3 s^{-1} y^{-1}), Aug ($\beta = -4.2$ m^3 s^{-1} y^{-1}), Sep ($\beta = -4.9$ m^3 s^{-1} y^{-1}) and Oct ($\beta = -3.0$ m^3 s^{-1} y^{-1}). Similar to MOF, the rate of decrease in mean monthly flow intensified post-1974 in the UAR for these months with the addition of Mar ($\beta = -1.2$ m^3 s^{-1} y^{-1}). Contrasts in increasing and

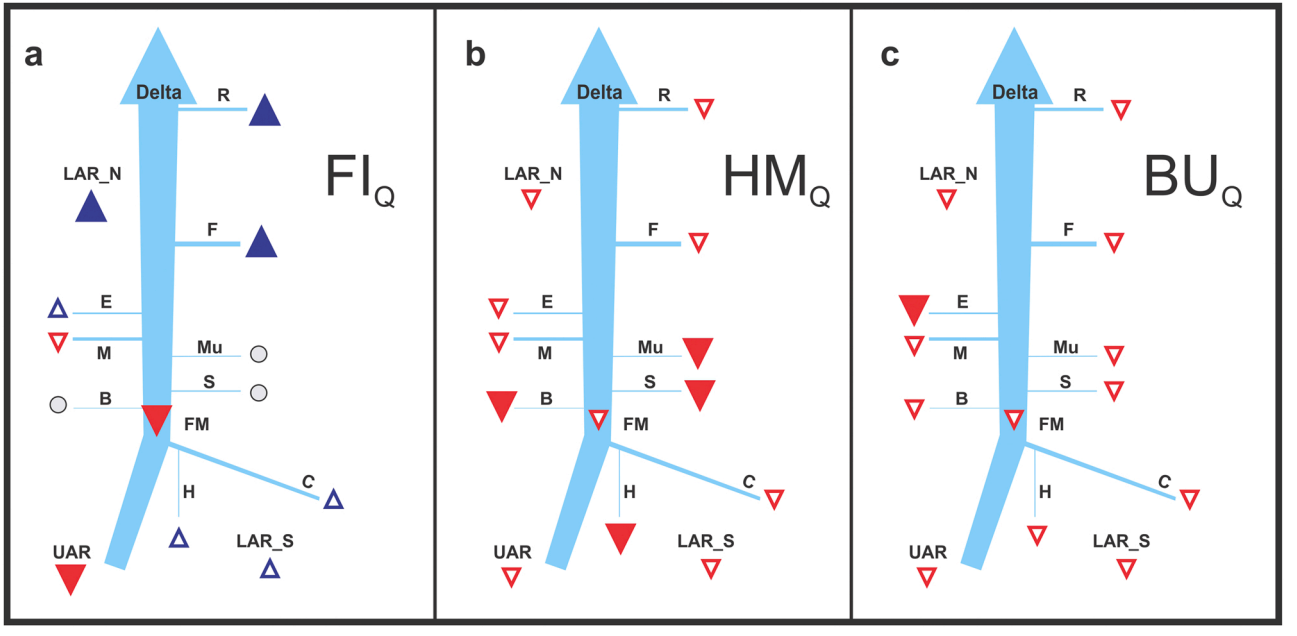

Fig. 7. Results for select trend analyses spanning 1974 – 2017: a) Flow at spring freshet initiation (FI_Q); b) Flow magnitude on day of peak backwater levels (HM_Q) on Athabasca River below Fort McMurray; c) Flow at spring breakup (BU_Q). Red triangles are decreasing and blue triangles are increasing tendencies, with significant trends ($p \leq 0.10$) depicted by filled in triangles, and grey circles depict a slope of zero. (For interpretation of the references to colour in this figure legend, the reader is referred to the web version of this article.)

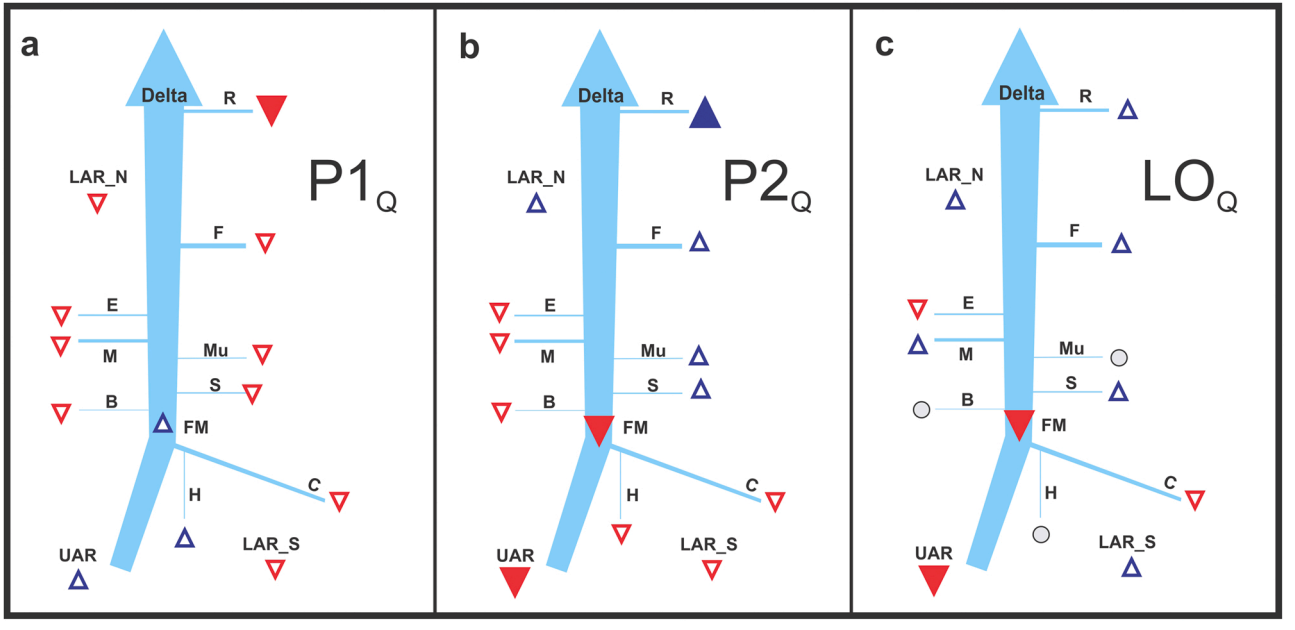

Fig. 8. Results for select trend analyses spanning 1974 – 2017: a) peak flow magnitude prior to June 1st ($P1_Q$); b) peak flow magnitude post -June 1st ($P2_Q$); c) open water minimum flow magnitude (LO_Q). Red triangles are decreasing and blue triangles are increasing tendencies, with significant trends ($p \leq 0.10$) depicted by filled in triangles, and grey circles depict a slope of zero. (For interpretation of the references to colour in this figure legend, the reader is referred to the web version of this article.)

decreasing tendencies in flow from the tributaries downstream in the LAR_N were observed. The LAR_N tributary contributions were insufficient to offset the significant decreases in flow passing FM and onwards to the delta for the months of Mar and Jul through Oct ($\beta = -1.0$; -9.9; -8.2; -8.8; & -4.7 m^3 s^{-1} y^{-1}, respectively). The declining Sep flows are highlighted in Fig. 6b, since it is a time of year when waterway depth is critical to access traditional hunting activities along the LAR and PAD waterways (Carver and Maclean, 2016). Overall, although there is a slight general decline in certain monthly mean flows since 1974 on the river mainstem (ie, UAR), with the combination of weak decreases or increases from various tributaries in the LAR appearing to moderate the rate of decline at the basin scale as compared to the larger decreases (β) in flow observed from the UAR over this period.

The relative contributions of the UAR and LAR to the overall basin flow varied by season and highlight the importance of contributions from the LAR to the PAD during the spring snow freshet and rainfall-dominated months. The relative mean flow contributions from the LAR were greatest during Mar through May ($\bar{X} = 44\%$, 41% and 37%, respectively), as well as Sep and Oct ($\bar{X} = 30$, 36%), but where lower during Jun through Aug ($\bar{X} = 25\%$, 22%, and 24%). Conversely, flow contributions from the UAR were greater during Jun through Aug ($\bar{X} = 75\%$, 78%, and 76%). For the LAR, increasing flow contribution tendencies were discerned for all months since 1974, with several months statistically significant (Mar $\beta = 0.31\%$ y^{-1}; Jul $\beta = 0.21\%$ y^{-1}; Sep $\beta = 0.27\%$ y^{-1}).

The centre of mass date (CM_d) for the 1974–2017 period occurred significantly earlier for flow emanating from the UAR ($\beta = -0.33$ d y^{-1}) and flowing by FM ($\beta = -0.30$ d y^{-1}). Downstream, the CM_d tended to arrive earlier over time in the LAR_S tributaries, which contrasts with the LAR_N tributaries (Fig. 6c). The overall results from analyses of broad March to October indicators reveal that flow declines have been largely driven by runoff generation from above the LAR region, as suggested in Peters et al. (2013), with potentially important shift in timing (date) of generation that may affect ice and open water period indicators.

4.3. Ice influenced period indicators

The date and magnitude of maximum backwater level prior to the loss of an ice cover was only available at FM; we thus used this date to examine the flow magnitude and relative flow contributions from all the tributaries on that day. The complete set of spring breakup metrics at FM ($\pm$ 1 SD; 1958–2017) include the dates of freshet initiation (FI_d: $\bar{X}$ April 7 $\pm$ 9 d), maximum water level affected by ice (HM_d: $\bar{X}$ = April 21 $\pm$ 6 d), and river ice breakup (BU_d: $\bar{X}$ = April 27 $\pm$ 5 d). No statistically significant ($p > 0.10$) trends were discerned for these three variables at FM, nor for the freshet and breakup dates for the UAR and LAR.

For both study time periods (from 1958 or 1974), the FI_Q emanating from the UAR area significantly decreased ($\beta = -0.68$ m^3 s^{-1} y^{-1}; $\beta = -1.37$ m^3 s^{-1} y^{-1}, respectively) (Fig. 7a). The opposite trends were observed for FI_Q in the downstream tributaries of the LAR region, with significant increases for the LAR_N ($\beta = 0.17$ m^3 s^{-1} y^{-1}) since 1974 - notably in the Ells, Firebag and Richardson Rivers ($\beta = 0.02$ m^3 s^{-1} y^{-1}: $\beta = 0.07$ m^3 s^{-1} y^{-1}; $\beta = -0.06$ m^3 s^{-1} y^{-1}; respectively).

General decreases in flow for HM_Q and BU_Q were observed from both the 1958 and 1974 periods for the UAR, and similar decreasing tendencies were also observed for all tributaries within the LAR (Figs. 7b and 7c). In particular, the LAR_S experienced significant decreases in HM_Q ($\beta = -2.13$ m^3 s^{-1} y^{-1}) and BU_Q ($\beta = -1.87$ m^3 s^{-1} y^{-1}) since 1958. Since 1974, significant decreases in HM_Q emerged for the Hangingstone, Beaver, Steepbank and Muskeg Rivers ($\beta = -0.06$ m^3 s^{-1} y^{-1}; $\beta = 0.01$ m^3 s^{-1} y^{-1}; $\beta = 0.12$ m^3 s^{-1} y^{-1}; $\beta = 0.07$ m^3 s^{-1} y^{-1}; respectively); while for BU_Q only the Ells River revealed noteworthy trends ($\beta = -0.22$ m^3 s^{-1} y^{-1}).

Of interest is the increasing relative role of LAR compared to UAR to the river mainstem at a time of year when ice-jam generated floods can occur. Generally, the UAR contributed the majority of flow to HM_Q ($\bar{X} = 74 \pm 11\%$) at FM, with the remainder emanating from the LAR_S ($\bar{X} = 26 \pm 11\%$). However, the decreases from the UAR correspond to concurrent increases from LAR_S regions in the relative amounts of flow driving HM_Q at FM since 1974. Further, although the proportion of flow from the LAR_N can range greatly – adding as little as ~8% in 2015 and up to 62% in 1974 ($\bar{X} = 25 \pm 13\%$) to the downstream mainstem on the day of HM_Q - the proportion of flow from the lower LAR_N to the overall basin flow has generally declined (ie, Mackay $\beta = -0.07\%$ y^{-1}; Steepbank $\beta < -0.02\%$ y^{-1}).

4.4. Open water period indicators

The date of peak spring flow ($P1_d$, May 17 $\pm$ 12.5 d) for water emanating from the UAR has generally occurred 10 days later compared to the LAR region. Overall, the date has been occurring later at FM since 1958 and 1974 ($\beta = 0.17$ d y^{-1}; $\beta = 0.42$ d y^{-1}). Post-1974 notable occurrences of later dates included the UAR ($\beta = 0.30$ d y^{-1}) and LAR_N ($\beta = 0.35$ d y^{-1}), with tributaries Hangingstone, Beaver, Ells, Muskeg and Firebag Rivers ($\beta = 0.24$, 0.25, 0.41, 0.33, and 0.41 d y^{-1}, respectively). For the considerably more variable date of summer peak flow ($P2_d$), the date for the UAR ($\bar{X}$ = July 5 $\pm$ 21 d) generally occurred earlier than for the LAR_S ($\bar{X}$ = July 10 $\pm$ 35 d) and LAR_N ($\bar{X}$ = July 19 $\pm$ 40 d) regions after 1974. Only the Beaver River ($\beta = -0.61$ d y^{-1}) exhibited a significant change.

Flow magnitude of peak spring $P1_Q$ and summer $P2_Q$ (both important for overbank flooding of deltaic channels) generally decreased since 1958 for the UAR, with a significant decreasing trend in $P1_Q$ for the LAR_S ($\beta = -2.85$ m^3 s^{-1} y^{-1}). Predominantly decreasing tendencies were found in $P1_Q$ post-1974 (ie, Richardson River $\beta = -0.12$ m^3 s^{-1} y^{-1}) (Fig. 8a and b). Later in the summer, the UAR experienced a significant decrease in $P2_Q$ ($\beta = -17.02$ m^3 s^{-1} y^{-1}), with apparent decreases in the LAR_S and from west bank tributaries of the LAR_N. However, $P2_Q$ on east bank tributaries generally increased post-1974, with a significant increase ($\beta = 0.99$ m^3 s^{-1} y^{-1}) for the Firebag River. On average, the UAR contributed the majority of the flow generating the $P1_Q$ ($\bar{X} = 81.1 \pm 7\%$) and $P2_Q$ ($\bar{X} = 89.9 \pm 5\%$) measured at FM over 1974–2017, with the LAR_S contributing the remainder of the flow. On the days of the $P1_Q$ and $P2_Q$ at FM, it was estimated that the river reach along LAR_N added an additional 19.3 $\pm$ 11% and 8.8 $\pm$ 7% to the peak flow passing FM, respectively.

Sustained high flows are important to replenish storage within the downstream delta lakes. The $P90_d$ for the UAR has occurred significantly earlier ($\beta = -0.41$ d y^{-1}) since 1974. The relative contribution of water to $P90_Q$ from the UAR to FM generally decreased; however, there was a general increase in contributions from the LAR_S and downstream additions from the LAR_N, with significant

increasing trends for the Firebag and Richardson Rivers, ($\beta = 0.04\%$ y^{-1}; $\beta = 0.01\%$ y^{-1}). The bulk of the flow driving $P90_Q$ at FM originated from upstream areas ($\bar{X} = 84.1 \pm 5\%$), with the LAR_N providing additional flow that augmented the magnitude arriving to the delta by an average of $13.6 \pm 5\%$.

The day of low flow (LO_d) generally occurred earlier ($p > 0.10$) for the UAR and LAR_S since 1974, culminating into a significant trend with earlier LO_d for the FM station ($\beta = -0.12$ d y^{-1}) (Fig. 8c). In contrast, the general trend of a later LO_d in the LAR_N ($p > 0.10$) is influenced by significantly later trends in the Beaver ($\beta = 0.94$ d y^{-1}) and Muskeg ($\beta = 0.64$ d y^{-1}) Rivers. A similar contrast in low flow magnitude (LO_Q) was noted, with LO_Q in the UAR significantly decreasing since 1958 ($\beta = -1.95$ m^3 s^{-1} y^{-1}) and 1974 ($\beta = -3.53$ m^3 s^{-1} y^{-1}). This result was reflected in the relative flow contributions on LO_d at FM, with an apparent declining trend for the UAR, apparent increasing trend for the LAR_S, and significantly increasing trend for the LAR_N ($\beta = 0.31\%$ y^{-1}). The UAR contributed the majority of the flow generating LO_Q ($\bar{X} = 73.2 \pm 8\%$) at FM, with the LAR_S contributing the difference. The LAR_N was estimated to have provided an additional $20.4 \pm 9\%$ of flow downstream of FM, revealing that the lower regions of the basin generally played a larger role in generating runoff to the PAD during low flow periods than during peak flows.

4.5. Potential causes of directional change and spatial divergence in runoff

Our results clearly highlighted the importance of basin geography and differential contributions to overall streamflow generation to the downstream delta, and identified variations across the ice-covered and open-water periods. Observed decreases in runoff from the UAR concomitant with no overall change in runoff from the LAR indicate that the relative proportion of runoff from the lower Athabasca Basin has been increasing since 1974. This study also revealed potentially divergent trends in runoff regimes between the UAR and LAR, as well as east versus west bank tributaries of the LAR_N. Factors that affect the partitioning of water over the landscape are important in determining the Athabasca River flow regimes, such as climate variability and change, and the interaction with basin geography (basin size, geology, landcover).

Air temperatures have been warming over the past century in the region (Bonsal and Cuell, 2017; Bush et al., 2019; Peters et al., 2013). Although Peters et al. (2013) found a significant increase in precipitation occurred over the 1913–2009 period ($\beta = 0.50$ mm y^{-1}), they also noted significant decreases for the 1958–2009 and 1976–2009 periods ($\beta =$ - 0.99 & -0.21 mm y^{-1}, respectively). This trend in basin scale precipitation is associated with a decline (-0.66 mm y^{-1}) in the winter snowpack over 1950–2010 (O'Neil et al., 2017). Similar to observations in the adjacent Peace River (Beltaos et al., 2006), the decline in snowpack and warming air temperatures across the Athabasca River basin partly explains the earlier timing and widespread decline of summer peak flows, and may have also influenced the relative contributions of tributary flow to BU_Q and HM_Q near FM. It is important to mention that in additional to regional influences outlined in this section, air temperature, precipitation and associated streamflow generation has been found to be correspond to broader, synoptic scale climate teleconnections, such as the Pacific Decadal Oscillation (PDO) and Pacific North American (PNA) indices, at least partially explaining the post mid-1970s flow declines observed from the headwaters (Peters et al., 2013; Rood et al., 2017, 2015; Sauchyn et al., 2015; Whitfield et al., 2010).

In a study of Standardized Precipitation Evapotranspiration Index (SPEI), Bonsal and Cuell (2017) noted a general tendency (-0.25 yr^{-1}) towards drier and warmer conditions over 1950–2009, with the rate of decrease in SPEI greatest for the middle portions of the basin (-0.40) and least for the LAR (-0.08). Bawden et al. (2014) presented data (see their Fig. 5) that appear to suggest that March to October precipitation amounts (1976–2010) decreased on west bank versus increased on east bank tributaries. The overall contrast in runoff water balance component tendencies in the UAR and LAR are similar to the observed spatially divergent runoff response in this study, such as observed increase in fraction LAR region to $P2_Q$ and contrasting east vs west bank LAR tributaries.

Runoff generation in the LAR was influenced by differences in landscape controls on water movement and balances as outlined in a stable isotope hydrograph separation study by Gibson et al. (2016). They found that the east bank tributaries (Steepbank, Muskeg, and Firebag Rivers) were generally groundwater-dominated runoff systems; whereas the west bank tributaries (Mackay and Ells River) that drain the Birch Mountains and Wabasca Lowlands, and the Clearwater River that drains the Canadian Shield, were found to be mostly surface-water dominated systems, mainly derived from peatlands and lakes. In parallel studies of lake isotope mass balance calculations in and around the LAR, Gibson et al., (2019, 2015) postulated that permafrost thaw enhanced runoff contributions to 14 of 50 lakes in the region (mostly the Birch Mountains). The loss of permafrost is therefore another potential influence on the amount of runoff generation, with Gibson et al. (2019) also proposing a permafrost thaw trajectory for bog dominated areas whereby water yields initially increase but then decreases as the frozen source waters are depleted, all of which could drive observed flow trends.

Across the Boreal Plains catchments of Alberta, the greatest long-term runoff (lowest evapotranspiration) was observed in basins dominated with peatland and conifer swamp land cover combined with a large percentage (>14%) cover of coarse textured surficial geology (Devito et al., 2017). In contrast, reductions in flow (higher evapotranspiration) were associated with hummocky moraine landforms and deciduous forestland cover. LAR tributaries included in their regional study showed that long-term runoff and runoff/-precipitation ratios were greater in two east bank (Steepbank = 0.27; Muskeg = 0.21) versus two west bank (Beaver = 0.19; Mackay = 0.17) tributaries. Peatland-swamps dominate the land cover in both the west and east bank tributaries (~49% ± 18% and 51% ± 24%, respectively), and runoff productivity is generally high in the region. However, gauged basins on the west bank, representative of the Wabasca lowlands, are dominated by fine textured glacial deposits (% coarse ~2% ± 2%) with a substantial coverage by hummocky moraine (~18% ± 6%). These land-cover characteristics limit west bank runoff production compared to tributaries of the east bank (Devito et al., 2017). East bank tributaries are located in the Athabasca plains fluvial depositional areas, with no hummocky moraine, and are characterized by large expanses of coarse glacial and aeolian deposits (29% ± 22%) and less productive pine conifer forests, potentially increasing runoff production and extending low flows, particularly during dry weather cycles (Devito, pers. comm.).

Differences in geology along the Athabasca Basin are also important in influencing the spatial response of rivers and relative LAR

flow contributions. Although peatlands have numerous negative feedbacks acting on future climate change (Waddington et al., 2015), west bank tributaries and regions with a predominance of fine textured substrate, hummock moraine landforms and deciduous forest may be more susceptible to climate warming (Devito et al., 2017; Schneider et al., 2016), as suggested by declining flow from UAR. In contrast, the east bank tributaries, the Richardson River and ungauged northern portion of the LAR, are located in areas dominated by coarse textured glacial fluvial and eolian deposits (Fenton et al., 2013). Regions with coarse texture soil and substrate are characterized by xeric ecosystem types (Jack Pine forest) with lower rates of evapotranspiration, promoting infiltration, groundwater recharge and regional runoff generation that is likely to persist under future climate change scenarios (Devito et al., In Prep; Schneider et al., 2016). For instance, contrary to Athabasca River basin-scale runoff, summer flows (1–4%) are estimated to increase under projected mid- and late-century climate change scenarios for the west bank Firebag tributary (Eum et al., 2017).

Extensive land-cover change (e.g. 35–55%) may play a larger role in affecting the hydrological regime than climate change in the Muskeg River basin (Eum et al., 2016). The effects of current oil-sands mining activity on runoff generation are difficult to assess given the multitudes of potential hydrological alterations that are not readily reported spatio-temporarily and difficult to model year-to-year and over the long term. For instance, in the landscape most heavily affected by mining activity (~17%), the 2015 Muskeg River hydrograph was estimated to have deviated from the baseline flow conditions: mean annual open-water (+2.1%), mean winter (+11.1%), maximum peak (−3.8%), and minimum (+4.6%) (RAMP, 2016). There would also have been changes in mean annual flow throughout development phases as illustrated by the Jackpine Mine Expansion environmental assessment, which described an increase ~1% during wetland drainage and overburden dewatering activities in 2012, a ~8% maximum reduction from close-circuit operations, and ~9% increase at closure of the mine (Shell Canada, 2007). The surface landscapes of other LAR tributaries are considerably less affected by mining activities (<2%; Table 1), with the flow regime expected to be less impacted than the illustrated Muskeg River.

Water allocation within the study basin has risen steadily since the 1960s, but is still < 5% of the total annual flow reaching the delta (eg, Fig. 5c) (AEP, 2019). According to the Lower Athabasca River Water Management Framework (GoA, 2015), the oil sands industry has a maximum cumulative allowable water extraction of 29 $m^3 s^{-1}$ from the Athabasca River when flow is ample (eg, summer time), reducing to 4.4 $m^3 s^{-1}$ when flow is restricted (eg, winter time) (AEP, 2019). In recent years, ~4 $m^3 s^{-1}$ on average has been extracted by the oil sands industry (AER, 2019), which is a small percentage of the mean annual flow, although nevertheless contributing to a cumulative reduction in flows reaching the delta (Fig. 5b). Anticipated climate change will likely change the relative importance of these allocations and the geography of the basin contributions, with Eum et al. (2017) projecting (2050s and 2080s) significant increases in spring flow (19–30% and 26–40%), decreases in summer flow (−8 to 0.6% and −2 to −8%), and increases in peak flows (2–18% and 12–19%) flow past FM on the Athabasca River mainstem. Furthermore, it can be suggested from the results of Eum et al. (2017) that the direction and magnitude of historical trends in the hydrological indicators may be reversed, continue as is or intensified over the next decades.

5. Summary and Conclusions

Understanding the availability of water in the Athabasca River basin is a matter of ongoing public concern in light of climate change, and with water use by oil and gas developments continuing to increase. Moreover, there is a need to develop an environmental flow framework for the downstream PAD that incorporates cold-regions hydrological indicators. Our novel analysis approach yielded new insights that should be considered in water management plans and decision making for this basin.

- A combined magnitude and relative flow contributions analysis by geography provides a clearer understanding of runoff generation change, in terms of opposing responses occurring within a basin.
- Landscape and geology partly explain potential causes of divergent responses of runoff generation leading to diverging responses to climate.
- Mean MOF over the past century did not exhibit a notable declining trend at FM, but significant declines were detected for the post-1958 and 1974 periods, the latter of which is largely driven by runoff generation originating from above the LAR oil-sands mining region.
- The timing of spring freshet initiation and river-ice breakup in the LAR basin has not changed significantly over the past half century. In line with the literature, there was a general decrease in the amount of water emanating from the upper regions for these two spring breakup indicators, with mixed results from the lower regions of the basin.
- Separating the open-water season into pre- and post-June 1st periods yielded results consistent with the literature but also new results. The magnitude of peak flow generally declined after 1958 in the UAR and LAR_S. However, while generally decreasing peak flows occurred in the pre-June 1st period throughout the LAR over 1974–2017, the post-June 1st open-water period experienced decreases from the UAR, LAR_S and the west bank of the LAR_N, with the east bank experiencing increasing peak flows. Similarly, open-water low flows decreased from upper regions and had a generally increasing tendency in the lower regions.
- The approach developed and applied in this study can be transferred to other cold region basins as it relies on information that can be readily obtained and/or generated. It is recommended that our approach be considered in future runoff generation studies with a goal of better understanding how basin geography affects hydro-ecological indicators known to influence river and deltaic ecosystems.

CRediT authorship contribution statement

DL Peters: Project management, Conceptualization, Data curation, Formal analysis, Investigation, Methodology, Visualization, Writing – original draft, Writing – review & editing. **D Watt**: Investigation, Writing – original draft. **K Devito**: Investigation, Writing – original draft, Writing – review & editing. **WA Monk**: Investigation, Writing – original draft, Writing – review & editing. **RR Shrestha**: Investigation, Writing – original draft, Writing – review & editing. **DJ Baird**: Investigation, Writing – original draft, Writing – review & editing.

Declaration of Competing Interest

The authors declare that they have no known competing financial interests or personal relationships that could have appeared to influence the work reported in this paper.

Acknowledgements

This project was supported by the Climate Change Adaptation Program of Environment and Climate Change Canada. We wish to thank Cydne Potter for help in drafting the maps.

Appendix A

Results from Mann-Kendall trend analyses. The Sen's slope (β) and P values are presented for specified time periods and sites of interest defined as: UAR- Upper Athabasca River; LAR_S - Lower Athabasca River South; LAR_N – Lower Athabasca River North; FM – Athabasca River just below Fort McMurray; B -Beaver River; M – Mackay River; E – Ells River; H – Hangingstone River; C- Clearwater River; S -Steepbank River; Mu – Muskeg River; F – Firebag River; and R – Richardson River.

See Appendix Tables A1-A24.

1974–2017																
	March		April		May		June		July		August		September		October	
Sites	β % y^{-1}	P	β % y^{-1}	P	β % y^{-1}	P	β % y^{-1}	P	β % y^{-1}	P	β % y^{-1}	P	β % y^{-1}	P	β % y^{-1}	P
UAR	-0.31	0.00	-0.12	0.53	0.02	0.92	-0.03	0.88	-0.21	0.07	-0.17	0.15	-0.27	0.10	-0.23	0.17
LAR	0.31	0.00	0.12	0.53	-0.02	0.92	0.03	0.88	0.21	0.07	0.17	0.15	0.27	0.10	0.23	0.17
LAR_S	0.15	0.01	0.08	0.46	0.01	0.97	0.04	0.54	0.11	0.10	0.10	0.12	0.14	0.07	0.13	0.27
LAR_N	0.17	0.00	0.08	0.38	-0.03	0.82	-0.01	0.95	0.09	0.10	0.06	0.11	0.15	0.03	0.13	0.08

Table A1
Mean March to October flow (MOF) magnitude.

	1912–2017		1958–2017		1974–2017	
Sites	β m^3 s^{-1} y^{-1}	P	β m^3 s^{-1} y^{-1}	P	β m^3 s^{-1} y^{-1}	P
AT	-0.31	0.54	-1.51	0.21	-2.47	0.15
FM	-0.87	0.26	-3.49	0.08	-3.45	0.19
UAR			-2.89	0.08	-4.05	0.09
LAR_S			-0.32	0.37	0.10	0.87
C			-0.30	0.41	0.12	0.88
H					-0.03	0.36
LAR_N					-0.02	0.98
B					-0.01	0.28
M					-0.06	0.63
E					-0.08	0.37
S					0.02	0.79
Mu					-0.01	0.75
F					0.17	0.31
R					0.03	0.33
Basin					-4.53	0.22

Table A2
Mean March to October flow (MOF) percentage contribution of total basin flow.

%	1974–2017	
Sites	β % y^{-1}	P
FM	-0.08	0.22
UAR	-0.19	0.07
LAR_S	0.12	0.08
LAR_N	0.08	0.22
Basin	0.19	0.07

Table A3
Monthly mean flow magnitude.

1958–2017																
	March		April		May		June		July		August		September		October	
Sites	β $m^3 s^{-1} y^{-1}$	P	β $m^3 s^{-1} y^{-1}$	P	β $m^3 s^{-1} y^{-1}$	P	β $m^3 s^{-1} y^{-1}$	P	β $m^3 s^{-1} y^{-1}$	P	β $m^3 s^{-1} y^{-1}$	P	β $m^3 s^{-1} y^{-1}$	P	β $m^3 s^{-1} y^{-1}$	P
FM	-0.30	0.40	-1.17	0.50	-4.19	0.20	-2.62	0.45	-6.47	0.06	-4.80	0.03	-5.90	0.00	-4.12	0.01
UAR	-0.34	0.26	-0.93	0.58	-2.64	0.29	-2.14	0.51	-5.76	0.06	-4.23	0.03	-4.87	0.00	-3.02	0.01
LAR_S	0.01	0.87	-0.30	0.42	-1.32	0.11	-0.34	0.66	0.15	0.80	-0.25	0.52	-0.61	0.30	-0.61	0.26
C	0.01	0.92	-0.29	0.44	-1.23	0.12	-0.34	0.70	0.24	0.73	-0.22	0.57	-0.58	0.31	-0.56	0.27

Table A4
Monthly mean flow percentage contribution.

1974–2017

	March		April		May		June		July		August		September		October	
Sites	β m^3 s^{-1} y^{-1}	P	β m^3 s^{-1} y^{-1}	P	β m^3 s^{-1} y^{-1}	P	β m^3 s^{-1} y^{-1}	P	β m^3 s^{-1} y^{-1}	P	β m^3 s^{-1} y^{-1}	P	β m^3 s^{-1} y^{-1}	P	β m^3 s^{-1} y^{-1}	P
FM	-1.20	0.05	-3.16	0.28	0.54	0.92	2.76	0.62	-10.46	0.05	-8.40	0.02	-8.78	0.00	-4.28	0.05
UAR	-1.20	0.01	-2.83	0.26	-1.22	0.71	2.90	0.71	-11.47	0.03	-7.91	0.01	-8.61	0.00	-4.53	0.02
LAR_S	-0.05	0.62	-0.40	0.54	0.63	0.72	0.64	0.52	0.26	0.83	-0.35	0.75	-0.77	0.45	-0.41	0.56
C	-0.05	0.59	-0.34	0.59	0.54	0.72	0.73	0.43	0.37	0.77	-0.32	0.77	-0.79	0.46	-0.30	0.68
H	0.00	0.65	-0.12	0.08	-0.10	0.63	-0.04	0.80	-0.09	0.52	-0.05	0.50	-0.07	0.60	-0.08	0.33
LAR_N	0.14	0.03	-0.63	0.32	0.33	0.88	0.03	0.97	0.47	0.49	-0.20	0.68	-0.02	0.99	0.17	0.87
B	0.00	0.38	-0.01	0.08	0.01	0.57	0.00	0.75	0.00	0.88	0.00	0.12	-0.01	0.18	0.00	0.35
M	0.00	0.71	-0.19	0.06	-0.08	0.83	-0.17	0.88	0.16	0.52	-0.02	0.88	-0.02	0.85	-0.02	0.80
E	0.01	0.04	-0.05	0.31	-0.13	0.48	-0.14	0.71	0.01	0.88	-0.05	0.52	-0.04	0.44	-0.03	0.59
S	0.00	0.88	-0.03	0.32	0.01	0.98	0.13	0.29	0.07	0.36	-0.02	0.69	-0.01	0.85	-0.01	0.69
Mu	0.00	1.00	-0.03	0.23	0.02	0.85	0.06	0.60	0.01	0.78	-0.02	0.24	-0.02	0.52	-0.04	0.43
F	0.04	0.06	-0.07	0.71	0.09	0.77	0.20	0.60	0.20	0.24	-0.01	0.94	0.09	0.63	0.12	0.54
R	0.04	0.04	-0.02	0.65	0.01	0.90	0.02	0.80	0.04	0.29	0.03	0.49	0.06	0.08	0.06	0.22
Basin	-1.04	0.10	-3.35	0.25	0.65	0.87	2.63	0.75	-9.85	0.06	-8.16	0.02	-8.89	0.01	-4.63	0.09

Table A5
Centre of mass (CM_d) date.

	1974–2017	
Sites	β d y^{-1}	P
FM	-0.30	0.02
UAR	-0.33	0.02
LAR_S	-0.12	0.63
C	-0.13	0.56
H	-0.18	0.61
LAR_N	0.08	0.77
B	-0.25	0.45
M	0.32	0.46
E	0.12	0.74
S	0.04	0.94
Mu	-0.17	0.64
F	0.07	0.78
R	0.17	0.20

Table A6
Spring Freshet initiation (FI_d) date.

	1958–2017		1974–2017	
Sites	β d y^{-1}	P	β d y^{-1}	P
FM	-0.02	0.83	0.14	0.35
UAR	0.00	1.00	0.21	0.22
LAR_S	-0.02	0.90	0.07	0.59
C	-0.02	0.86	0.06	0.63
H			0.02	0.92
LAR_N			-0.06	0.65
B			0.13	0.25
M			-0.11	0.49
E			-0.08	0.54
S			-0.12	0.33
Mu			0.00	0.90
F			0.12	0.33
R			0.06	0.83

Table A7
Spring Freshet initiation (FI_Q) flow magnitude.

	1958–2017		1974–2017	
Sites	β m^3 s^{-1} y^{-1}	P	β m^3 s^{-1} y^{-1}	P
FM	-0.42	0.26	-1.24	0.04
UAR	-0.68	0.05	-1.37	0.01
LAR_S	0.07	0.35	0.08	0.60
C	0.05	0.47	0.07	0.68
H			0.00	0.70
LAR_N			0.17	0.03
B			0.00	0.37
M			-0.01	0.65
E			0.02	0.10
S			0.00	0.87
Mu			0.00	0.85
F			0.07	0.01
R			0.06	0.01

Table A8
Date of maximum backwater stage influenced by ice (HM_d).

	1958–2017		1974–2017	
Sites	β d y^{-1}	P	β d y^{-1}	P
FM	-0.01	0.91	0.10	0.43

Table A9
Flow on date of maximum backwater stage influenced by ice (HM_Q).

	1958–2017		1974–2017	
Sites	β m^3 s^{-1} y^{-1}	P	β m^3 s^{-1} y^{-1}	P
FM	-6.09	0.18	-5.79	0.31
UAR	-4.01	0.34	-3.27	0.41
LAR_S	-2.13	0.01	-1.29	0.20
C	-2.11	0.03	-1.12	0.29
H			-0.06	0.04
LAR_N			-0.95	0.28
B			-0.01	0.09
M			-0.24	0.24
E			-0.04	0.43
S			-0.12	0.09
Mu			-0.07	0.10
F			-0.20	0.17
R			-0.07	0.41

Table A10
Percentage of flow for HM_Q measured at FM for the UAR and LAR_S regions, while the LAR_N and its tributaries are additional % contribution to FM magnitude.

	1974–2017	
Sites	β % y^{-1}	P
FM	–	–
UAR	-0.04	0.83
LAR_S	0.04	0.83
C	0.01	0.99
H	0.00	0.19
LAR_N	-0.11	0.46
B	0.00	0.49
M	-0.07	0.04
E	-0.01	0.44
S	-0.02	0.03
Mu	0.00	0.55
F	0.02	0.76
R	-0.04	0.33

Table A11
Date of river ice Breakup (BU_d).

	1958–2017		1974–2017	
Sites	β d y^{-1}	P	β d y^{-1}	P
FM	-0.03	0.40	0.07	0.19
UAR	-0.03	0.40	0.07	0.19
LAR_S	-0.06	0.26	0.09	0.39
C	-0.06	0.26	0.09	0.39
H			0.11	0.37
LAR_N			0.10	0.15
B			0.18	0.15
M			0.13	0.16
E			0.13	0.15
S			0.14	0.09
Mu			0.02	0.86
F			0.12	0.16
R			-0.01	0.91

Table A12
Flow magnitude on date of Breakup (BU_Q).

	1958–2017		1974–2017	
Sites	β m^3 s^{-1} y^{-1}	P	β m^3 s^{-1} y^{-1}	P
FM	-2.24	0.55	-4.10	0.49
UAR	-0.66	0.73	-2.89	0.50
LAR_S	-1.87	0.05	-0.46	0.69
C	-1.59	0.05	-0.08	0.93
H			-0.01	0.92
LAR_N			-1.20	0.25
B			-0.01	0.51
M			-0.48	0.15
E			-0.22	0.09
S			-0.06	0.50
Mu			-0.10	0.13
F			-0.20	0.80
R			-0.12	0.12

Table A13
Date of spring peak daily flow magnitude ($P1_d$).

	1958–2017		1974–2017	
Sites	β d y^{-1}	P	β d y^{-1}	P
FM	0.17	0.05	0.42	0.00
UAR	0.08	0.25	0.35	0.01
LAR_S	0.00	0.93	0.11	0.47
C	0.00	0.94	0.10	0.51
H			0.24	0.09
LAR_N			0.30	0.02
B			0.25	0.08
M			0.25	0.11
E			0.41	0.02
S			0.23	0.11
Mu			0.33	0.02
F			0.24	0.09
R			0.11	0.32

Table A14
Spring period peak flow magnitude ($P1_Q$).

	1958–2017		1974–2017	
Sites	β m^3 s^{-1} y^{-1}	P	β m^3 s^{-1} y^{-1}	P
FM	-4.69	0.30	1.63	0.82
UAR	-3.37	0.43	1.81	0.80
LAR_S	-2.85	0.02	-0.40	0.82
C	-2.68	0.02	-0.30	0.82
H			0.05	0.79
LAR_N			-1.58	0.44
B			-0.01	0.86
M			-0.41	0.51
E			-0.20	0.38
S			-0.03	0.79
Mu			-0.04	0.80
F			-0.30	0.62
R			-0.12	0.09

Table A15
Percentage of flow for $P1_Q$ measured at FM for the UAR and LAR_S regions, while the LAR_N and its tributaries are additional % contribution to FM magnitude.

	1974–2017	
Sites	β % y^{-1}	P
FM	–	–
UAR	0.09	0.37
LAR_S	-0.09	0.37
C	-0.12	0.19
H	0.00	0.79
LAR_N	-0.13	0.28
B	0.00	0.80
M	-0.03	0.45
E	-0.02	0.26
S	-0.01	0.44
Mu	0.00	0.63
F	-0.04	0.25
R	-0.01	0.17

Table A16
Date of summer peak daily flow magnitude ($P2_d$).

	1958–2017		1974–2017	
Sites	β d y^{-1}	P	β d y^{-1}	P
FM	-0.15	0.33	-0.36	0.24
UAR	-0.16	0.31	-0.37	0.20
LAR_S	0.14	0.33	0.08	0.75
C	0.15	0.35	0.08	0.78
H			0.14	0.83
LAR_N			0.40	0.32
B			-0.61	0.08
M			0.26	0.42
E			0.12	0.69
S			0.09	0.75
Mu			-0.51	0.23
F			0.13	0.68
R			0.50	0.13

Table A17
Summer period peak flow magnitude ($P2_Q$).

	1958–2017		1974–2017	
Sites	β m^3 s^{-1} y^{-1}	P	β m^3 s^{-1} y^{-1}	P
FM	-10.04	0.22	-15.47	0.09
UAR	-7.62	0.21	-17.02	0.06
LAR_S	-1.06	0.32	-0.69	0.71
C	-1.03	0.23	-0.34	0.83
H			-0.09	0.67
LAR_N			0.01	1.00
B			-0.10	0.14
M			-0.64	0.46
E			-0.18	0.57
S			0.42	0.13
Mu			0.05	0.88
F			0.99	0.08
R			0.12	0.20

Table A18
Percentage of flow for $P2_Q$ measured at FM for the UAR and LAR_S regions, while the LAR_N and its tributaries are additional % contribution to FM magnitude.

	1974–2017	
Sites	β % y^{-1}	P
FM	–	–
UAR	-0.02	0.80
LAR_S	0.02	0.80
C	0.03	0.74
H	0.00	0.68
LAR_N	0.01	0.93
B	0.00	0.59
M	0.00	1.00
E	0.00	0.92
S	0.00	0.56
Mu	0.00	0.56
F	0.00	0.75
R	0.01	0.05

Table A19
Date of 90 day mean flow magnitude ($P90_d$).

	1958–2017		1974–2017	
Sites	β d y^{-1}	P	β d y^{-1}	P
FM	-4.79	0.15	-0.42	0.11
UAR	-3.40	0.15	-0.41	0.09
LAR_S	-0.52	0.33	-0.16	0.54
C	-0.48	0.35	-0.15	0.56
H			0.00	0.98
LAR_N			0.04	0.79
B			-0.25	0.09
M			0.12	0.63
E			-0.09	0.78
S			0.04	0.86
Mu			-0.05	0.76
F			0.00	0.98
R			0.11	0.71

Table A20
90 day mean flow magnitude ($P90_Q$).

	1958–2017		1974–2017	
Sites	β m^3 s^{-1} y^{-1}	P	β m^3 s^{-1} y^{-1}	P
FM	-4.79	0.15	-4.67	0.34
UAR	-3.40	0.15	-5.22	0.21
LAR_S	-0.52	0.33	0.33	0.74
C	-0.48	0.35	0.43	0.63
H			-0.05	0.35
LAR_N			-0.42	0.69
B			-0.01	0.33
M			-0.19	0.43
E			-0.13	0.41
S			-0.03	0.77
Mu			-0.05	0.59
F			0.19	0.31
R			0.02	0.66

Table A21
Percentage of flow for $P90_Q$ measured at FM for the UAR and LAR_S regions, while the LAR_N and its tributaries are additional % contribution to FM magnitude.

	1974–2017	
Sites	β % y^{-1}	P
FM	–	–
UAR	-0.10	0.14
LAR_S	0.09	0.21
C	0.10	0.19
H	0.00	0.41
LAR_N	0.07	0.43
B	0.00	0.88
M	0.00	0.83
E	-0.01	0.69
S	0.01	0.22
Mu	0.00	0.63
F	0.04	0.09
R	0.01	0.03

Table A22
Date of mean daily low flow magnitude (LO_d).

	1958–2017		1974–2017	
Sites	β d y^{-1}	P	β d y^{-1}	P
FM	0.00	0.43	-0.12	0.02
UAR	0.00	0.48	-0.17	0.19
LAR_S	0.16	0.64	-0.40	0.44
C	0.15	0.66	-0.39	0.42
H			0.22	0.62
LAR_N			0.40	0.21
B			0.94	0.04
M			0.31	0.54
E			0.71	0.17
S			0.08	0.89
Mu			0.64	0.09
F			0.44	0.16
R			-0.26	0.39

Table A23
Mean daily low flow magnitude (LO_Q).

	1958–2017		1974–2017	
Sites	β m^3 s^{-1} y^{-1}	P	β m^3 s^{-1} y^{-1}	P
FM	-2.79	0.03	-4.65	0.02
UAR	-1.95	0.05	-3.53	0.03
LAR_S	-0.19	0.50	0.04	0.95
C	-0.18	0.53	-0.02	1.00
H			0.00	0.59
LAR_N			0.10	0.74
B			0.00	0.65
M			0.02	0.48
E			-0.01	0.77
S			0.01	0.32
Mu			0.00	0.95
F			0.02	0.77
R			0.02	0.37

Table A24
Percentage of flow for LO_Q measured at FM for the UAR and LAR_S regions, while the LAR_N and its tributaries are additional % contribution to FM magnitude.

	1974–2017	
Sites	β % y^{-1}	P
FM	–	–
UAR	-0.15	0.32
LAR_S	0.15	0.32
C	0.15	0.30
H	0.00	0.96
LAR_N	0.31	0.03
B	0.00	0.56
M	0.01	0.69
E	0.00	0.87
S	0.01	0.25
Mu	0.01	0.56
F	0.12	0.00
R	0.06	0.00

References

ABMI, 2020. Alberta Biomonitoring Institute [WWW Document]. Human Footprint Products. URL ⟨https://abmi.ca/home/data-analytics/da-top/da-product-overview/Human-Footprint-Products⟩.

AEP, 2019. Athabasca River historical water allocations - Alberta Environment and Parks. URL ⟨https://albertawater.com/images/FactsAndInfo/Alberta/alloc/alloc-natflow3.jpg⟩.

AER, 2019. Alberta Energy Regulator oil sands water use data.

Alexander, A.C., Chambers, P.A., 2016. Assessment of seven Canadian rivers in relation to stages in oil sands industrial development, 1972-2010. Environ. Rev. 24, 484–494.

Bawden, A.J., Linton, H.C., Burn, D.H., Prowse, T.D., 2014. A spatiotemporal analysis of hydrological trends and variability in the Athabasca River region, Canada. J. Hydrol. 509, 333–342. https://doi.org/10.1016/j.jhydrol.2013.11.051.

Beltaos, S., Prowse, T., Bonsal, B., MacKay, R., Romolo, L., Pietroniro, A., Toth, B., 2006. Climatic effects on ice-jam flooding of the Peace-Athabasca Delta. Hydrol. Process. 20, 4031–4050. https://doi.org/10.1002/hyp.6418.

Bonsal, B., Peters, D.L., Seglenieks, F., Rivera, A., Berg, A., 2019. Changes in freshwater availability across Canada. In: Bush, E., Lemmen, D.S. (Eds.), Canada's Changing Climate Report. Government of Canada, Ottawa, ON, pp. 261–342.

Bonsal, B., Shrestha, R.R., Dibike, Y., Peters, D.L., Spence, C., Mudryk, L., Yang, D., 2020. Western Canadian freshwater availability: current and future vulnerabilities. Environ. Rev. https://doi.org/10.1139/er-2020-0040.

Bonsal, B.R., Cuell, C., 2017. Hydro-climatic variability and extremes over the Athabasca River basin: historical trends and projected future occurrence. Can. Water Resour. J. 42, 315–335. https://doi.org/10.1080/07011784.2017.1328288.

Bothe, R.A., 1982. Athabasca River Study Historical Natural flows. Alberta Environment Report, Edmonton, Alberta, Canada, pp. 1912–1980.

Botter, G., Basso, S., Rodriguez-Iturbe, I., Rinaldo, A., 2013. Resilience of river flow regimes. PNAS 110, 12925–12930. https://doi.org/10.1073/pnas.1311920110.

Bronaugh, D., Werner, A.T., 2019. ZYP Package.

Bürger, G., 2017. On trend detection. Hydrol. Process. 31, 4039–4042. https://doi.org/10.1002/hyp.11280.

Burn, D.H., Hag Elnur, M.A., 2002. Detection of hydrologic trends and variability. J. Hydrol. 255, 107–122. https://doi.org/10.1016/S0022-1694(01)00514-5.

Burn, D.H., Sharif, M., Zhang, K., 2010. Detection of trends in hydrological extremes for Canadian watersheds. Hydrol. Process. 24, 1781–1790. https://doi.org/10.1002/hyp.7625.

Bush, E., Gillett, N., Bonsal, B., Cohen, S., Derksen, C., Flato, G., Greenan, B.J.W., Sherperd, M., Zhang, X., 2019. Executve Summary, in: Canada's Climate Change Report. Environment and Climate Change Canada, Ottawa, ON.

Carver, M., Maclean, B., 2016. Community-Based Water-Depth Monitoring in the Peace-Athabasca Delta: Insights and Evaluation. Prepared by Aqua Environmental Associates for Athabasca Chipewyan First Nation and Mikisew Cree First Nation, Nelson, British Columbia, Canada.

Chen, Z., Grasby, S.E., 2014. Reconstructing river discharge trends from climate variables and prediction of future trends. J. Hydrol. 511, 267–278. https://doi.org/10.1016/j.jhydrol.2014.01.049.

de Rham, L., Dibike, Y., Beltaos, S., Peters, D., Bonsal, B., Prowse, T., 2020. A Canadian river ice database from national hydrometric program archives. Earth Syst. Sci. Data Discuss. 1–43. https://doi.org/10.5194/essd-2020-29.

Devito, K.J., Hokanson, K.J., Moore, P.A., Kettridge, N., Anderson, A.E., Chasmer, L., Hopkinson, C., Lukenbach, M.C., Mendoza, C.A., Morissette, J., Peters, D.L., Petrone, R.M., Silins, U., Smerdon, B., Waddington, J.M., 2017. Landscape controls on long-term runoff in subhumid heterogeneous Boreal Plains catchments. Hydrol. Process. 31, 2737–2751. https://doi.org/10.1002/hyp.11213.

Downing, D.J., Pettapiece, W.W., 2006. Natural regions and subregions of Alberta: Natural Regions Committee (No. Publication No. T/852.T). Government of Alberta.

ECCC, 2020. HYDAT Water Survey Data Products. URL ⟨https://www.canada.ca/en/environment-climate-change/services/water-overview/quantity/monitoring/survey/data-products-services.html⟩.

Environment Canada, 2004. Dams, Reservoirs and Flow Regulation, NWRI Scientific Assessment Report Series No. 3 and ACSD Science Assessment Series No. 1. Environment Canada, Burlington, Ontario.

Eum, H.-I., Dibike, Y., Prowse, T., 2017. Climate-induced alteration of hydrologic indicators in the Athabasca River Basin, Alberta, Canada. J. Hydrol. 544, 327–342. https://doi.org/10.1016/j.jhydrol.2016.11.034.

Eum, H.-I., Dibike, Y., Prowse, T., 2016. Comparative evaluation of the effects of climate and land-cover changes on hydrologic responses of the Muskeg River, Alberta, Canada. J. Hydrol.: Reg. Stud. 8, 198–221. https://doi.org/10.1016/j.ejrh.2016.10.003.

Fenton, M.M., Waters, E.J., Pawley, S.M., Atkinson, N., Utting, D.J., McKay, K., 2013. Surficial geology of Alberta MAP, 601, Scale, 1, 1.

Gibson, J.J., Birks, S.J., Moncur, M., 2019. Mapping water yield distribution across the South Athabasca Oil Sands (SAOS) area: Baseline surveys applying isotope mass balance of lakes. J. Hydrol.: Reg. Stud. 21, 1–13. https://doi.org/10.1016/j.ejrh.2018.11.001.

Gibson, J.J., Birks, S.J., Yi, Y., Vitt, D.H., 2015. Runoff to boreal lakes linked to land cover, watershed morphology and permafrost thaw: a 9-year isotope mass balance assessment. Hydrol. Process. 29, 3848–3861. https://doi.org/10.1002/hyp.10502.

Gibson, J.J., Yi, Y., Birks, S.J., 2016. Isotope-based partitioning of streamflow in the oil sands region, northern Alberta: towards a monitoring strategy for assessing flow sources and water quality controls. J. Hydrol.: Reg. Stud. 5, 131–148.

GoA, 2019. Governmetn of Alberta - Oil Sands Information. URL ⟨https://www.alberta.ca/about-oil-sands.aspx⟩.

GoA, 2015. Surface Water Quantity Management Framework for the Lower Athabasca River. Alberta Environment and Sustainable Resource Development, Government of Alberta, Edmonton, Alberta, Canada.
Kendall, M.G., 1975. Rank Correlation Methods. Charles Griffin, London, UK.
Kompanizare, M., Petrone, R.M., Shafii, M., Robinson, D.T., Rooney, R.C., 2018. Effect of climate change and mining on hydrological connectivity of surficial layers in the Athabasca Oil Sands Region. Hydrol. Process. 32, 3698–3716. https://doi.org/10.1002/hyp.13292.
Mann, H.B., 1945. Non-parametric test against trend. Econometrika 13, 245–259.
Monk, W.A., Compson, Z.G., Armanini, D.G., Orlofske, J.M., Curry, C.J., Peters, D.L., Crocker, J.B., Baird, D.J., 2018. Flow velocity–ecology thresholds in Canadian rivers: a comparison of trait and taxonomy-based approaches. Freshw. Biol. 63, 891–905. https://doi.org/10.1111/fwb.13030.
Monk, W.A., Peters, D.L., Baird, D.J., 2012. Assessment of ecologically relevant hydrological variables influencing a cold-region river and its delta: the Athabasca River and the Peace–Athabasca Delta, northwestern Canada. Hydrol. Process. 26, 1827–1839. https://doi.org/10.1002/hyp.9307.
Monk, W.A., Peters, D.L., Curry, R.A., Baird, D.J., 2011. Quantifying trends in indicator hydroecological variables for regime-based groups of Canadian rivers. Hydrol. Process. 25, 3086–3100. https://doi.org/10.1002/hyp.8137.
Neill, C.R., Evans, B.J., 1979. Synthesis of surface water hydrology (No. AOSERP Report 60), Prep. for the Alberta Oil Sands Environmental Research Program by Northwest Hydraulic Consultants Ltd.
NRBS, 1996. North. Rivers Basins Study - Rep. Minist.
O'Neil, H.C.L., Prowse, T.D., Bonsal, B.R., Dibike, Y.B., 2017. Spatial and temporal characteristics in streamflow-related hydroclimatic variables over western Canada. Part 1: 1950–2010. Hydrol. Res. 48, 915–931. https://doi.org/10.2166/nh.2016.057.
Peters, D.L., Atkinson, D., Monk, W.A., Tenenbaum, D.E., Baird, D.J., 2013. A multi-scale hydroclimatic analysis of runoff generation in the Athabasca River, western Canada. Hydrol. Process. 27, 1915–1934. https://doi.org/10.1002/hyp.9699.
Peters, D.L., Caissie, D., Monk, W.A., Rood, S.B., St-Hilaire, A., 2016. An ecological perspective on floods in Canada. Can. Water Resour. J. 41, 288–306. https://doi.org/10.1080/07011784.2015.1070694.
Peters, D.L., Monk, W.A., Baird, D.J., 2014. Cold-regions Hydrological Indicators of Change (CHIC) for ecological flow needs assessment. Hydrol. Sci. J. 59, 502–516. https://doi.org/10.1080/02626667.2013.835489.
Peters, D.L., Prowse, T.D., 2006. Generation of streamflow to seasonal high waters in a freshwater delta, northwestern Canada. Hydrol. Process. 20, 4173–4196. https://doi.org/10.1002/hyp.6425.
R Development Core Team, 2016. R: A Language and Environment for Statistical Computing. R Foundation for Statisti-cal Computing, Vienna.
RAMP, 2018. Regional Aquatic Monitoring Program. URL ⟨http://www.ramp-alberta.org/RAMP.aspx⟩.
RAMP, 2016. Regional Aquatics Monitoring in support of the Joint Oil Sands Monitoring Plan Final 2015 Program Report (Prepared for Alberta Monitoring Evaluation and Reporting Agency). Prepared by Hatfield Consultants, Kilgour and Associates Ltd and Western Resource Solutions.
Rasouli, K., Hernández-Henr&iacute M.A., Quez, Déry, S.J., 2013. Streamflow input to Lake Athabasca, Canada. Hydrol. Earth Syst. Sci. 17, 1681–1691. https://doi.org/10.5194/hess-17-1681-2013.
Richter, B.D., Baumgartner, J.V., Powell, J., Braun, D.P., 1996. A method for assessing hydrologic alteration within ecosystems. Conserv. Biol. 10, 1163–1174. https://doi.org/10.1046/j.1523-1739.1996.10041163.x.
Rood, S.B., Kaluthota, S., Philipsen, L.J., Rood, N.J., Zanewich, K.P., 2017. Increasing discharge from the Mackenzie River system to the Arctic Ocean. Hydrol. Process. 31, 150–160. https://doi.org/10.1002/hyp.10986.
Rood, S.B., Stupple, G.W., Gill, K.M., 2015. Century-long records reveal slight, ecoregion-localized changes in Athabasca River flows. Hydrol. Process. 29, 805–816. https://doi.org/10.1002/hyp.10194.
Sauchyn, D.J., St-Jacques, J.-M., Luckman, B.H., 2015. Long-term reliability of the Athabasca River (Alberta, Canada) as the water source for oil sands mining. PNAS 112, 12621–12626. https://doi.org/10.1073/pnas.1509726112.
Schindler, D.W., Donahue, W.F., 2006. An impending water crisis in Canada's western prairie provinces. Proc. Natl. Acad. Sci. U.S.A. 103 https://doi.org/10.1073/pnas.0601568103.
Schneider, R., Stelfox, J., Boutin, S., Wassel, S., 2003. Managing the cumulative impacts of land uses in the Western Canadian sedimentary basin: a modeling approach. Conserv. Ecol. 7, 8.
Schneider, R.R., Devito, K., Kettridge, N., Bayne, E., 2016. Moving beyond bioclimatic envelope models: integrating upland forest and peatland processes to predict ecosystem transitions under climate change in the western Canadian boreal plain. Ecohydrology 9, 899–908. https://doi.org/10.1002/eco.1707.
Sen, P.K., 1968. Estimates of the regression coefficient based on Kendall's Tau. J. Am. Stat. Assoc. 63, 1379–1389.
Seneka, M., 2002. Lower Athabasca River Hydrologic routing modelling (A report prepared for Environmental Assurance). Alberta Environment. Edmonton,, Alberta, Canada.
Shell Canada, 2007. Environmental Impact Assessment Aquat. Resour. Appl. Approv. Jackpine Mine Expans. Proj. Pierre River Mine Proj. Submitt. Alta. Energy Uti. Board Alta. Environ. Shell Can. Ltd. Volume 4A 2007.
Squires, A.J., Westbrook, C.J., Dubé, M.G., 2010. An approach for assessing cumulative effects in a model river, the Athabasca River basin. Integr. Environ. Assess. Manag. 6, 119–134. https://doi.org/10.1897/IEAM_2008-081.1.
Timoney, K.P., 2013. The Peace-Athabasca Delta: Portrait of a Dynamic Ecosystem. The University of Alberta Press, Edmonton, Alberta, Canada.
TNC, 2007. User's manual for the indicators of hydrologic alteration (IHA) software. The Nature Conservancy, Charlottesville, Viginia, USA.
UNESCO, 2017. Reactive Monitoring Mission (RMM) to Wood Buffalo National Park, Canada. Mission Report March 2017. UNESCO World Heritage Centre - WHC International Union for Conservation of Nature (IUCN).
Waddington, J.M., Morris, P.J., Kettridge, N., Granath, G., Thompson, D.K., Moore, P.A., 2015. Hydrological feedbacks in northern peatlands. Ecohydrology 8, 113–127. https://doi.org/10.1002/eco.1493.
Whitfield, P.H., Moore, R.D., Fleming, S.W., Zawadzki, A., 2010. Pacific decadal oscillation and the hydroclimatology of western Canada - review and prospects. Can. Water Resour. J. 35, 1–28.
Woynillowicz, D., Severson-Baker, C., 2006. Down to the Last Drop. The Pembina Institute, Drayton Valley, Alberta, Canada.
Zeiringer, B., Seliger, C., Greimel, F., Schmutz, S., 2018. River hydrology, flow alteration, and environmental flow. In: Schmutz, S., Sendzimir, J. (Eds.), Riverine Ecosystem Management: Science for Governing Towards a Sustainable Future. Springer International Publishing, Cham, pp. 67–89. https://doi.org/10.1007/978-3-319-73250-3_4.
Zhang, X., Vincent, L.A., Hogg, W.D., Niitsoo, A., 2000. Temperature and precipitation trends in Canada during the 20th century. Atmos.-Ocean 38, 395–429. https://doi.org/10.1080/07055900.2000.9649654.
Zhang, X., Zwiers, F.W., 2004. Comment on "applicability of prewhitening to eliminate the influence of serial correlation on the Mann-Kendall test" by Sheng Yue and Chun Yuan Wang. Water Resour. Res. 40. https://doi.org/10.1029/2003WR002073.